Bioreactivity of dissolved organic carbon in ponds of the ice-wedge polygonal tundra

Thomas Pacoureau[1,2,3], Milla Rautio[2,3,4], Isabelle Laurion[1,2,3]

[1]Laboratoire de limnologie nordique, Centre Eau Terre Environnement, Institut national de la recherche scientifique, Québec, QC, G1K 9A9, Canada
[2]Centre for northern studies, Université Laval, Québec, QC, G1V 0A6, Canada
[3]Interuniversity research group in limnology, Université de Montréal, Montréal, QC, H3C 3J7, Canada
[4]Laboratoire des sciences aquatiques, Département des sciences fondamentales, Université du Québec à Chicoutimi, Chicoutimi, QC, G7H 281, Canada

Correspondence to: Thomas Pacoureau (thomas.pacoureau@gmail.com)

Abstract. The role of ponds in transforming dissolved organic matter (DOM) within landscapes affected by permafrost thawing remains poorly understood, despite their potential importance in carbon cycling. Ice-wedge degradation in polygonal landscapes creates diverse pond types through various hydro-morphological processes. We hypothesized that this pond diversity generates DOM of varying bioreactivity. To test this, we conducted a 188-day bioassay using water from 15 ponds in northeastern Canada, representing the main geomorphological types characteristic of this widespread arctic landscape. Using optical spectroscopy and carbon quantification, we examined the relationship between DOM properties and bioreactivity, and conducted a parallel nutrient-addition bioassay to assess potential inorganic nitrogen and phosphorus limitations. Results show that a significant proportion of dissolved organic carbon (DOC) was available to bacterioplankton during summer (33% decomposed after 97 days). Contrary to our hypothesis, and despite variations in DOM composition, no difference in DOC loss was observed among the three pond categories studied (erosive ice-wedge trough ponds, stable ice-wedge trough ponds, and coalescent polygon ponds), indicating comparable bioavailable DOC pools. Moreover, nutrient addition did not significantly enhance DOC loss or decay coefficients, suggesting that bacterial decomposition depends primarily on the bioavailability of organic carbon. This was further supported by a positive correlation between DOC loss and tryptophan-like fluorophores, a marker of bioavailable DOM, suggesting that DOM released by cyanobacterial mats and other autochthonous producers may be more readily utilized by bacteria than DOM derived from peaty soils. These findings highlight the importance of freshly produced organic matter in regulating carbon cycling in polygonal tundra ponds, with implications for the fate of carbon released from thawing permafrost soils.

1 Introduction

Accelerated warming in the Arctic is driving the thaw and erosion of ice-rich permafrost, mobilizing vast reservoirs of previously frozen organic carbon (Liljedahl et al., 2016; Olefeldt et al., 2016; Nitze et al., 2018). A fraction of this carbon is released as dissolved organic matter (DOM) into inland waters (Abbott et al., 2015; Vonk et al., 2015b; Zhang et al., 2017),

where it accumulates in tundra ponds—ubiquitous features that comprise up to 95% of water bodies in regions such as the Canadian High Arctic, the Lena Delta in Siberia, and the Barrow Peninsula in Alaska (Muster et al., 2013). These ponds can form through thermokarst processes, including ground ice melt and ice-wedge degradation, which create interconnected networks of troughs and basins in the widespread polygonal tundra. Beyond acting as recipients for biodegradable permafrost-derived DOM (Vonk et al., 2015a), they host dynamic primary producer communities, including mosses, graminoids (Magnússon et al., 2020), phytoplankton, and benthic cyanobacterial mats (Rautio et al., 2011), which contribute to autochthonous DOM production. While tundra ponds (< 1000 m²) are recognized for their role in greenhouse gas exchange (Lougheed et al., 2020; Karlsson et al., 2021; Prėskienis et al., 2021), their role in transforming DOM derived from thawing soils, growing vegetation, and local primary producers remains poorly constrained, limiting our ability to predict Arctic carbon feedbacks under climate warming.

The source and chemical composition of DOM are key determinants of its bioreactivity (Abbott et al., 2014), but linking bioreactivity to specific DOM fractions is challenging due to its chemical complexity and diverse, seasonally shifting sources. In permafrost regions, these sources include organic compounds leached from thawing permafrost and its overlying active layer, as well as compounds produced by aquatic plants, benthic or planktonic algae, and bacterioplankton (Wauthy et al., 2018; Ma et al., 2019; Abbott et al., 2014). Absorption and fluorescence spectroscopy are valuable tools for characterizing the biogeochemical cycling of DOM in aquatic systems (Ateia et al., 2017; Stubbins et al., 2014; McCallister et al., 2018), but the bioreactivity of the "colored" DOM (CDOM) and fluorescent DOM (FDOM) fractions is not yet fully understood. The protein-like fluorescent fraction of DOM can be either consumed or produced during dark incubation of lake water (Berggren et al., 2020; Guillemette and del Giorgio, 2012), yet it remains closely linked to the bioavailability of DOM in surface waters, as demonstrated by a large-scale study of boreal lakes (Lapierre and del Giorgio, 2014). In Canada's organic permafrost deposits, Fouché et al. (2020) highlighted the release of protein-like FDOM due to active layer thickening and permafrost erosion, while cyanobacterial mats, mosses, and aquatic plants have also been identified as significant sources of these compounds in thaw ponds in similar deposits (Pacoureau et al., 2025). Understanding the fate of DOM entering thaw ponds and identifying the biogeochemical drivers of its bioreactivity is essential for refining regional carbon budgets and predicting Arctic catchment response to climate warming.

In addition to releasing potentially bioavailable DOM, permafrost thaw increases concentrations of inorganic nitrogen (N) and phosphorus (P) in surface waters (Vonk et al., 2015b; Fouché et al., 2020; Tank et al., 2020; Pacoureau et al., 2025). Enhanced N and P availability can stimulate bacterial growth and increase dissolved organic carbon (DOC) turnover rates (Mann et al., 2014; Allesson et al., 2020; Berggren et al., 2023). These macronutrients, especially P, have been shown to regulate bacterioplankton growth in temperate and boreal surface waters, often in conjunction with organic carbon (Smith and Prairie, 2004; Berggren et al., 2010; Vidal et al., 2011). This pattern of P limitation appears consistent across oligotrophic lakes in subarctic and Arctic regions (Granéli et al., 2004; Rodríguez et al., 2013). However, the extent to which nutrients influence DOC decomposition in high-DOM thaw ponds remains uncertain. In nutrient-poor permafrost thaw streams, adding inorganic N and P has been shown to double DOC turnover (Textor et al., 2019). Similar additions to waters from thermokarst features—

varying in ambient DOC and nutrient levels—nearly doubled the amount of rapidly decomposed DOC (i.e., DOC lost within 10 days) but had no effect on total DOC degraded over 40 days (Abbott et al., 2014). The influence of nutrient availability on bacterial DOC decomposition likely varies across the heterogeneous ponds of polygonal tundra landscapes, which exhibit substantial variability in morphology, thermokarst erosion intensity, vegetation colonization, and water transparency—factors that collectively modulate the availability of bioreactive carbon and nutrients to bacteria (Pacoureau et al., 2025; Prėskienis et al., 2021, 2024). Experimental studies are therefore needed to predict how thawing permafrost will influence bacterial DOC decomposition and mineralization.

In this study, we assessed DOM bioreactivity in the water column of ponds in landscapes with degrading ice-wedge polygons, underlain by organic-rich permafrost that formed concurrently with sediment accumulation (syngenetic permafrost). The three pond categories found in this landscape are: (1) eroding ice-wedge trough (eIWT) ponds; (2) stable ice-wedge trough (sIWT) ponds; and (3) coalescent polygon (CP) ponds. We incubated water samples for 188 days under dark, oxygenated conditions, with replicates amended with inorganic N and P to simulate nutrient-replete conditions. We hypothesized that (i) eIWT ponds would experience greater DOC loss than stable pond typess(sIWT and CP ponds), due to higher inputs of bioavailable DOC from permafrost erosion and surrounding soils, and (ii) nutrient addition would not increase DOC turnover rates across all pond categories, since these systems typically receive elevated N and P inputs relative to bioavailable allochthonous organic carbon, based on previous findings (Pacoureau et al., 2025). This study aims to provide empirical evidence about how permafrost thaw ponds process DOM, thereby improving predictions of carbon cycling and biogeochemical responses in rapidly changing Arctic landscapes.

2 Materials and methods

2.1 Study site and ponds

Bylot Island is located in the eastern Canadian Arctic, within the boundaries of Sirmilik National Park (73°09′ N, 79°58′ W) (**Fig. 1**). The study site lies in the Qarlikturvik Valley (~20 km²) on the western plain of the island. The valley features numerous lakes and ponds, surrounded by patches of both dry and wet tundra. Low- and high-centered polygons occur in organic-rich Holocene peaty-loess deposits (1.6–27% OC in the upper meter; Prėskienis, 2022) with excess pore ice. Collectively, these soils store an estimated 1,654 Tg C in the top meter, with an average OC stock of 82 kg C m^{-2} (Ola et al., 2022). In these deposits, the thickness of the active layer typically varies from 30 to 70 cm (Allard et al., 2024). Climatic data for the period 1994–2019 indicate an average annual temperature of −14.4°C, with total precipitation over the three summer months (June–August) averaging just 78 mm (CEN, 2020). According to the Circumpolar Arctic Vegetation Map, the site is classified as “Graminoid, prostrate dwarf-shrub, forb tundra” (Walker et al., 2005). Vegetation in wet sections of the studied polygons was dominated by sedges (e.g., *Eriphorum scheuchzeri* Hoppe, *Carex aquatilis* Walhenb.), grasses (e.g., *Arctagrostis latifolia* Griseb., *Dupontia fischeri* Nees, *Pleuropogon sabinei* R. Br.), carpets of fen mosses (e.g., *Aulocomnium* spp.), and submerged brown mosses (mainly *Drepanocladus* spp.) (Bilodeau et al., 2013). Drier environments such as polygon ridges

and the surrounding hummocky tundra host more diverse communities, with dwarf shrubs (e.g., *Salix arctica* Pall., *Cassiope tetragona* (L.) D. Don) being particularly abundant.

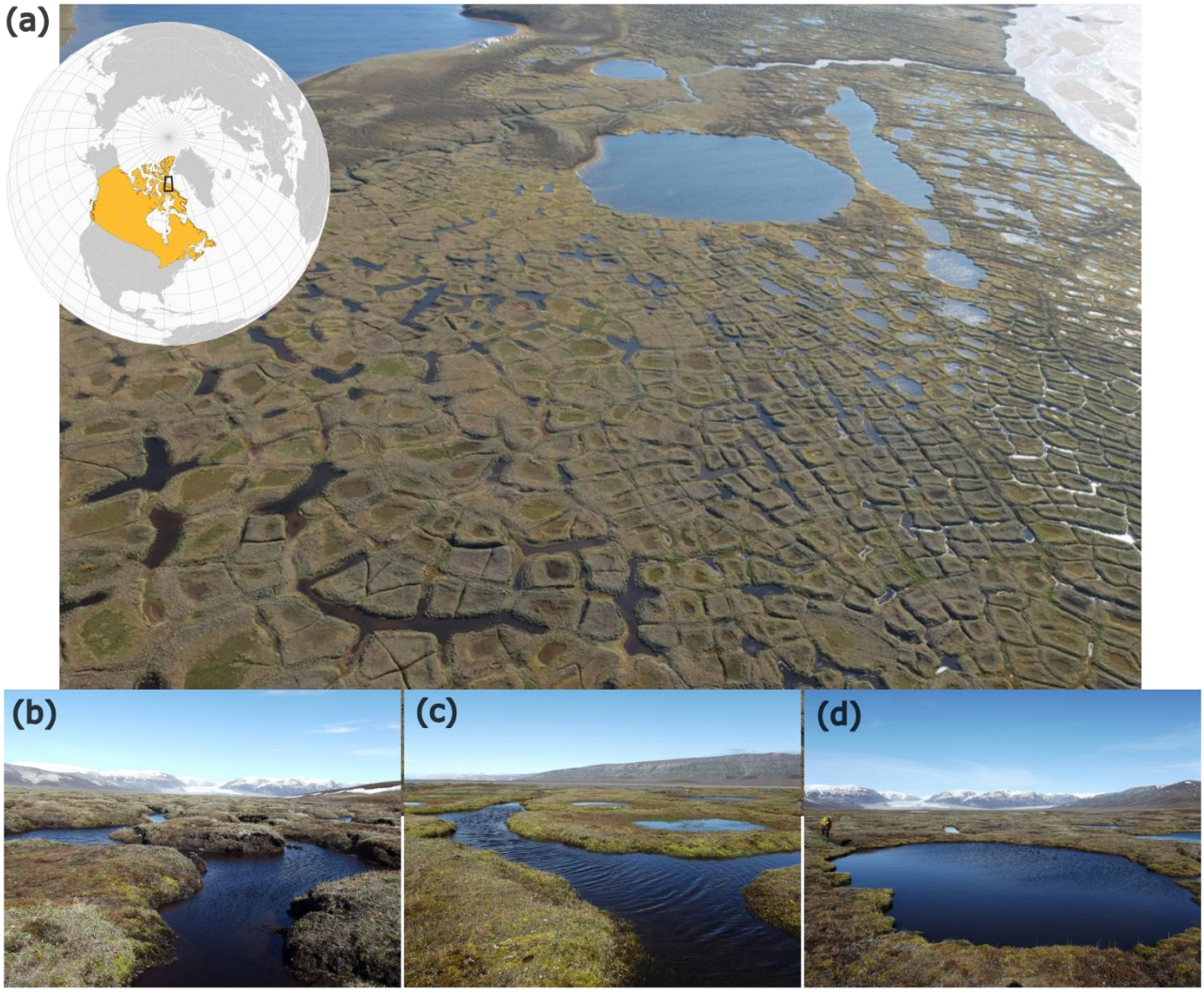

Figure 1: (a) Location of the study area and aerial view of the valley featuring an ice-wedge polygon complex (© Isabelle Laurion). (b-d) Photographs of representative ponds: (b) an erosive ice-wedge trough pond, (c) a stable ice-wedge trough pond, and (d) a coalescent polygon pond (© Thomas Pacoureau).

Ponds with surface area ranging from 26 to 997 m² (median: 178 m²) were selected to capture the biogeochemical variability characteristic of small waterbodies found in ice-wedge polygonal landscapes. Using the classification used by Pacoureau et al. (2025), we sampled five ponds from each of the three above-mentioned categories (**Fig. 1**). In brief, eIWT ponds are elongated, water-filled troughs that form above melting ice-wedges surrounding high-centered polygons. These ponds are characterized by bank erosion, dark-brown water, and a lack of emergent vegetation. As these ponds gradually accumulate sediments and

organic matter and are colonized by sedges and bryophytes, ice-wedge degradation slows, leading to the transition of eIWT ponds into sIWT ponds. However, certain geomorphological conditions can generate sIWT ponds directly upon inception, bypassing the eIWT stage (though they may evolve into eIWT ponds later). CP ponds, on the other hand, develop from soil subsidence in polygonal terrain, resulting from the merging of multiple ponds. CP ponds typically have a circular shape and a flat bottom. They are characterized by transparent waters, relatively steep banks that inhibit sedge establishment, and dense benthic cyanobacterial mats. All studied ponds are very shallow (< 1.5 m) and freeze completely to the bottom from late September to mid-June.

2.2 Sampling

A total of 15 ponds were sampled on July 27, 2017. Temperature and dissolved oxygen in the ponds were measured with a YSI multiparameter probe (Yellow Springs, OH, USA), and pH was measured using a PCSTestr 35 multiparameter probe (Oakton, VA, USA). Subsequently, two liters of water were collected from ~20 cm below the surface at the deepest point of each pond, using a peristaltic pump attached to a laminar sampler (see Fig. S3 in Matveev et al., 2019). Samples were stored in polycarbonate bottles and placed in a cooler until processing at the field station within 2.5 hours.

2.3 Bioassay

We conducted incubation experiments using water samples collected from 15 ponds (one sample per pond, without replication). Samples were filtered through pre-combusted Grade D glass-fiber filters (2.7 μm nominal retention, Whatman) to eliminate the need for an inoculation step and to remove crustacean grazers and most nanoflagellate bacterivores while retaining the natural bacterial community. Finer filters (0.2–0.7 μm pore size) tend to retain a large number of bacterial cells (Dean et al., 2018), particularly particle-attached bacteria. Such bacteria are abundant in thaw ponds and can account for over 50% of the total bacterial population and biomass production (Breton et al., 2009; Deshpande et al., 2016; Roiha et al., 2015). Additionally, using smaller pore size filters to remove bacterivores may disrupt the microbial loop and alter nutrient remineralization during prolonged incubations. By contrast, the larger 2.7 μm pore size yields DOC degradation dynamics that more closely approximate *in situ* conditions.

Filtered samples were incubated in 1-L polycarbonate bottles with a 20% air headspace, and maintained in darkness at 15°C to simulate heterotrophic microbial activity. Although this temperature is approximately 5°C higher than the average surface water temperature at the time of sampling (daytime mean ± 1σ at 20 cm depth = 10 ± 1°C, **Table 1**), it was selected to standardize conditions across experiments.

To assess the potential effect of nutrient limitation on bacterial DOM decomposition, we ran a parallel series of incubations with nutrient-replete samples. Pond water was amended with sodium nitrate ($NaNO_3$), ammonium chloride (NH_4Cl), and monopotassium phosphate (KH_2PO_4) to raise ambient NO_3^-–NH_4^+ and PO_4^{3-} concentrations by 80 μM and 10 μM, respectively. Because initial nutrient concentrations could not be measured prior to the bioassay, addition levels followed Vonk et al. (2015a) to ensure nutrient-replete conditions according to Redfield stoichiometry.

Incubation bottles were loosely capped and gently agitated every two days. At the start of incubation and on days 8, 15, 29, 71, 97 and 188, aliquots were collected for DOC, DOM absorbance and fluorescence, and flow cytometry analyses. Additional unfiltered aliquots were collected prior to the start of incubation for total phosphorus (TP), total nitrogen (TN), and chlorophyll *a* (Chl*a*; used as a proxy for algal biomass) analyses. Upon completion of the bioassay, the remaining water volume in the bottles exceeded half of the initial volume.

2.4 DOM reactivity

DOC loss was expressed as both the reduction in concentration (mg L^{-1}) and as a percentage of the initial DOC concentration, measured at days 29, 97, and 188 of the incubation. These time points include the typical duration of bioassays (one month) as well as extended incubation periods. Aliquots for DOC analysis were filtered through pre-combusted GF75 glass fiber filters (0.3 µm nominal retention, Advantec) and stored at 4°C in pre-combusted amber borosilicate glass vials, following acidification with sulfuric acid to a pH of approximately 2. Samples were analyzed for DOC concentrations within six months of collection using an Aurora 1030W TOC analyser (OI Analytical, College Station, TX, USA) following persulfate digestion (EPA Method 415.3). Blanks were prepared on each sampling day by filtering ultrapure water (Milli-Q®), and all measured DOC concentrations were below the detection limit of 0.1 mg C L^{-1}.

To describe DOC decomposition dynamics, we compared four commonly used models: a linear model (Eq. 1), an exponential decay model (Eq. 2), an exponential decay model with a residual DOC pool (Eq. 3), and the gamma reactivity continuum model (Eq. 4) (as in e.g., Koehler et al., 2012):

$$\frac{DOC_t}{DOC_0} = 1 - k \tag{1}$$

where k is the DOC decay rate (day^{-1}).

$$\frac{DOC_t}{DOC_0} = e^{-kt} \tag{2}$$

where t is the incubation time (days).

$$\frac{DOC_t}{DOC_0} = R + (1 - R)e^{-kt} \tag{3}$$

where R is the fraction of the initial DOC that is refractory (or non-decomposable) under the experimental conditions (unitless).

$$\frac{DOC_t}{DOC_0} = \left(\frac{\alpha}{\alpha + t}\right)^{\upsilon} \tag{4}$$

where α (days) and υ (unitless) are the two parameters of the Gamma distribution used in the reactivity continuum model (see below). Models were fitted to the relative DOC loss over time (DOC_t / DOC_0) for each incubation unit using R Statistical Software v4.3.3 (R Core Team, 2024). Linear models were applied using the "lm" function, while nonlinear models were fitted using the "nls" function, both from the built-in *stats* package. A two-pool exponential decay model was also considered, but it could not be fitted due to convergence issues.

Model selection was based on the sum of Akaike weights and the root mean square error (RMSE) calculated for each DOC decomposition time course. Akaike weights, derived from the corrected Akaike Information Criterion (AICc), reflect the probability of each model being the best among the set. RMSE was used to assess goodness-of-fit, with lower values indicating better model performance. It is important to note that the parameters estimated by each model depend on their underlying assumptions. Both the linear and exponential decay models provide decay coefficients (k, day^{-1}), while the exponential decay model with a residual pool also estimates the fraction of DOC that is not degraded. In contrast, the reactivity continuum model yields two parameters: the rate parameter a, representing the average lifetime of the more reactive compounds, and the shape parameter υ, reflecting the shape of the initial reactivity distribution.

2.5 DOM optical analysis

Samples for DOM optical analyses were filtered through pre-combusted grade F glass fiber filters and stored at 4°C without headspace or preservative until analysis the following day, thereby minimizing the loss of labile compounds during storage. Absorbance was measured on a dual-beam Cary 100 UV-Vis spectrometer (Agilent, Santa Clara, USA), with ultrapure water serving as the blank. Scans were collected at room temperature from 200 to 800 nm in 1 nm increments, and spectra were baseline-corrected by subtracting the mean absorbance between 790 and 800 nm. Napierian absorption coefficients were calculated by multiplying absorbance by 2.303 and dividing by the path length of the quartz cuvette (0.01 m). The absorption coefficient at 320 nm (a_{320}, in m^{-1}) was used as a proxy for CDOM concentration, the specific ultraviolet absorbance at 254 nm ($SUVA_{254}$, in L mg C^{-1} m^{-1}) served as an indicator of DOM aromaticity (Weishaar et al., 2003), and the spectral slope coefficient between 275 and 295 nm (S_{285}, in nm^{-1}) was used as a proxy of DOM molecular weight (Helms et al., 2008).

To further characterize DOM at the start of the bioassay, excitation-emission matrices (EEMs) were generated using a Cary Eclipse spectrofluorometer (Agilent, Santa Clara, CA, USA). Excitation wavelengths ranged from 240 to 450 nm in 5 nm increments, and emission wavelengths ranged from 300 to 560 nm in 2 nm increments. EEMs were corrected according to Murphy et al. (2013) using the FDOMcorr toolbox v1.6, and analyzed, along with other samples from the study site, using parallel factor analysis (PARAFAC). The model was developed using 385 samples: 276 pond waters, 35 plant leachates, 26 permafrost soil leachates, 20 transition layer soil leachates, and 28 active layer soil leachates. This dataset included the 15 to incubation samples at ambient nutrient concentrations. The resulting component loadings were subsequently applied to all remaining incubation samples across all time points and nutrient conditions. For details regarding the PARAFAC modeling procedure, see Pacoureau et al. (2025). Eight components were resolved (**Fig. S1**). Based on comparison with reference spectra in the OpenFluor repository (www.openfluor.org; Murphy et al., 2014), we identified four "terrestrial" humic-like fluorescence

components (HT1–4), two "microbial" humic-like fluorescent components (HM1–2), and two protein-like components (P1–2). The concentration of each fluorescent component (*Ci*) in a given sample was expressed as its maximum intensity (F_{max}) in Raman units (RU), while total fluorescence (F_{tot}) was calculated as the sum of all *Ci*.

2.6 Nutrient and chlorophyll *a* analyses

TN and TP were determined in unfiltered samples using colorimetric methods. TN was measured on a QuickChem 8000 automated ion analyzer (Lachat Instruments, Milwaukee, WI, USA) following digestion of the samples (EPA Method 353.2; detection limit of 4 µg L^{-1}), and TP was measured on an Astoria 2 analyzer (Astoria-Pacific, Clackamas, OR, USA) (EPA Method 365.3; detection limit of 0.7 µg L^{-1}). Chlorophyll *a* (Chl*a*) was extracted with hot ethanol, and its concentration was determined fluorometrically before and after acidification to correct for pheopigments (Nusch, 1980).

2.7 Bacterial abundance

Samples for bacterial counts were preserved with glutaraldehyde (1% final concentration) and stored in cryogenic vials at −80°C until analysis. Bacterial cell abundances (BA, in cell mL^{-1}) were determined using an Accuri C6+ flow cytometer (BD Biosciences, Franklin Lakes, NJ, USA). Prior to analysis, samples were thawed and sonicated in an ice bath for 5 minutes (Sonifier SFX150, Branson Ultrasonics Corporation, Brookfield, CT, USA) with pulses of 0.1 s s^{-1} at 50% duty cycle (~10 W). This step aimed to ensure that most particle-attached bacteria were included in the cytometric counts. Aliquots were stained in the dark with 25 µl of SYBR Green I (2.5X final concentration; Invitrogen S7563) for 15 minutes. Samples were then analyzed in triplicate for 1 minute each at a slow flow rate, with a green fluorescence (FL1) intensity threshold set at 700 and acquisition in log mode. If necessary, samples were diluted with distilled water to keep the count rate below 1000 events per second to prevent coincidence. The cytometer's flow rate was calibrated on each day of analysis by running a BD Trucount™ Absolute Counting Tube (total volume 2 ml) in triplicate at the beginning and end of the session. All samples received 1 µm yellow-green fluorescent microspheres as a particle size standard. Manual gating was performed using BD Accuri C6+ software to discriminate bacteria from other particles using FL1 versus red fluorescence (FL3) plots, and to delineate bacterial populations using the side-scatter (SSC) versus FL1 plots.

2.8 Statistical analyses

All statistical analyses were performed in R version 4.3.3 (R Core Team, 2024). One-way analysis of variance (ANOVA), followed by Tukey's honest significant difference (Tukey HSD) tests for multiple comparisons, was used to assess differences in *in situ* mean temperature and pH among pond categories, and mean DOC, TP, TN, and Chl*a* concentrations, BA, and optical properties among pond categories at the start of the bioassay.

To assess the effects of pond category (between-subject factor) and incubation day (within-subject factor) on DOC loss at days 29, 97, and 188, we conducted a two-way mixed-measures ANOVA for unamended samples using the "anova_test" function from the *rstatix* package (v0.7.0; Kassambara, 2023). This analysis was repeated to test the effects of pond category (between-

subject factor) and nutrient addition (within-subject factor) on DOC loss at the end of the bioassay (day 188). Mixed ANOVAs were followed by post-hoc pairwise t-tests with Bonferroni correction for multiple comparisons (implemented in the base *stats* package in R). Before conducting the ANOVAs, residual diagnostic plots were visually inspected to verify the assumptions of normality and homoscedasticity. Degrees of freedom were adjusted using the Greenhous-Geisser correction to avoid inflated F-ratios when the sphericity assumption was violated for mixed ANOVAs (i.e., Mauchly's test $P < 0.05$).

An exponential decay model with a residual DOC pool was fitted to all data within a nonlinear mixed-effects modeling framework, using the "nlme" function from the *nlme* package (Pinheiro and Bates, 2023). This approach is well-suited for data with a hierarchical structure, such as DOC decomposition time series with samples nested within ponds. In the model, pond category (three levels: eIWT, sIWT and CP) and nutrient addition (two levels: ambient and nutrient-replete) were treated as fixed effects, while pond identity was included as a random effect to account for pseudoreplication for both k and the residual DOC fraction. Model parameters were estimated via maximum likelihood. Differences in fixed effects were tested by ANOVA, followed by post hoc pairwise comparisons using the "emmeans" function from the *emmeans* package, with P values adjusted using the Tukey method (Lenth et al., 2025).

To identify which variables measured during the initial characterization of the assayed waters best explained variation in DOC loss at days 97 and 188, as well as DOC decay coefficients, we performed multiple linear regression analyses using pooled unamended samples from all 15 ponds. Potential explanatory variables included TP, TN, Chl*a*, a_{320}, $SUVA_{254}$, S_{285}, and the fluorescence intensity of each PARAFAC component (F_{max}). All humic-like PARAFAC components were highly correlated with a_{320} (Spearman's $\rho > 0.9$), so we excluded them from the set of explanatory variables. All possible models were generated using the remaining predictors (a_{320}, $SUVA_{254}$, Chl*a*, TN, TP, P1, and P2), and the best models were selected based on AICc, retaining those within 5 AICc units of the top-ranked model. Models were ranked according to their Akaike weights using the "lm" function (base *stats* package) and the "dredge" function (*MuMIn* package; Bartoń, 2024). The quality of the retained models was assessed using diagnostic plots and examination of residual heteroscedasticity, while the significance of regression coefficients in each model was assessed using t-test.

3 Results

3.1 Initial biogeochemical characteristics of pond waters

We detected differences in DOC and TP concentrations among pond categories at the start of the bioassay (**Table 1**). Mean DOC and TP concentrations in eIWT ponds were 1.3 and 1.6 times higher, respectively, compared to concentrations in CP ponds. In contrast, mean concentrations of TN and Chl*a* did not differ among pond categories. Although bacterial abundance showed slight variations among pond categories, mean values remained within the same order of magnitude.

DOM was more colored in eIWT ponds, with CDOM (expressed as a_{320}) decreasing by twofold and fourfold in sIWT and CP ponds, respectively. $SUVA_{254}$ values indicated a decreasing proportion of aromatic structures in DOM from eIWT to CP ponds,

with sIWT ponds showing intermediate values. The slope S_{285} suggested a lower apparent DOM molecular weight in CP ponds compared to ice-wedge trough ponds.

DOM was more fluorescent in eIWT ponds, with FDOM (expressed as F_{tot}) being 1.7 and 2.4 times higher, respectively, compared to sIWT and CP ponds (**Table 1**). PARAFAC analysis revealed the dominance of terrestrial humic-like components in the ponds (**Fig. 2**), particularly component HT1. The mean fluorescence of all terrestrial humic-like components decreased between eIWT and sIWT or CP ponds (for HT2, eIWT > sIWT > CP). Microbial humic-like components showed higher mean fluorescence in eIWT ponds compared to sIWT and CP ponds. The tryptophan-like component (P1) generally dominated the total amino acid-like fluorescence in our dataset (range 0.25–0.58 RU). P1 and the tyrosine-like component (P2) showed no differences in mean fluorescence among pond categories.

Table 1: Initial characterization of the assayed waters. Ranges are presented for each parameter, with mean ± SE (n = 5) for each pond category. Mesological conditions include temperature, pH, dissolved organic carbon (DOC), total phosphorus (TP), total nitrogen (TN), chlorophyll *a* (Chl*a*) as a proxy for phytoplankton biomass, bacterial abundance (BA), dissolved organic matter (DOM) absorption coefficient at 320 nm (a_{320}), specific ultraviolet absorbance at 254 nm ($SUVA_{254}$), spectral slope estimated between 275 and 295 nm (S_{285}), and total fluorescence intensity (F_{tot}). Within each row, different letters represent significant differences between pond categories according to Tukey's HSD test ($P < 0.05$).

	Range	Eroding ice-wedge troughs (eIWT) ponds	Stabilized ice-wedge troughs (sIWT) ponds	Coalescent polygon (CP) ponds	One-way ANOVA, $F_{(2, 12)}$
Physicochemical parameters (*in situ*, 20 cm below surface)					
Temperature (°C)	8.1–11.6	10.2 ± 0.3	10.4 ± 0.5	9.6 ± 0.5	F = 0.790, P = 0.476, η^2 = 0.12
pH	6.7–9.5	7.3 ± 0.2	8.0 ± 0.3	8.5 ± 0.4	F = 3.09, P = 0.083, η^2 = 0.34
Nutrients					
DOC (mg L^{-1})	10.6–18.5	17.4 ± 0.2^{a}	14.8 ± 1.1^{ab}	13.3 ± 1.2^{b}	F = 4.43, P = 0.036, η^2 = 0.42
TP (µg L^{-1})	16.0–52.1	43.3 ± 1.9^{a}	28.6 ± 6.1^{ab}	25.8 ± 3.0^{b}	F = 5.29, P = 0.023, η^2 = 0.47
TN (µg L^{-1})	753–1198	1010 ± 31	924 ± 75	1003 ± 75	F = 0.560, P = 0.580, η^2 = 0.09
DOC:TN molar ratio	11–23.7	20.2 ± 0.9^{a}	18.8 ± 1.2^{ab}	15.6 ± 1.2^{b}	F = 4.30, P = 0.039, η^2 = 0.42
DOC:TP molar ratio	659–2071	1080 ± 56	1586 ± 257	1440 ± 180	F = 2.00, P = 0.177, η^2 = 0.25
Biological parameters					
Chl*a* (µg L^{-1})	0.3–12.6	2.3 ± 0.6	1.9 ± 1.0	4.6 ± 2.1	F = 0.920, P = 0.420, η^2 = 0.13
BA (x 10^6 cell ml^{-1})	0.9–4.4	2.56 ± 0.67	1.08 ± 0.08	1.68 ± 0.22	F = 3.29, P = 0.073, η^2 = 0.35
DOM optical properties					
a_{320} (m^{-1})	11.3–74.0	60.8 ± 3.9^{a}	33.0 ± 5.9^{b}	14.8 ± 7.2^{c}	F = 26.4, P = 4.01 ×10^{-5}, η^2 = 0.82
$SUVA_{254}$ (L mg C^{-1} m^{-1})	1.3–3.2	3.4 ± 0.1^{a}	2.42 ± 0.3^{a}	1.53 ± 0.1^{b}	F = 5.37, P = 0.022, η^2 = 0.47
S_{285} (nm^{-1})	0.012–0.024	0.013 ± 0^{a}	0.016 ± 0.001^{a}	0.021 ± 0.001^{b}	F = 19.8, P = 1.59 × 10^{-4}, η^2 = 0.77
F_{tot} (RU)	1.7–6.3	5.8 ± 0.2^{a}	3.4 ± 0.4^{b}	2.4 ± 0.5^{b}	F = 21.5, P = 1.08 × 10^{-4}, η^2 = 0.78

3.2 DOC loss

Under ambient nutrient concentrations, DOC loss ranged between 0.3–7.1 mg L^{-1} (2–41% of initial DOC) across all samples and incubation times. No difference in mean DOC loss was detected among pond categories for absolute concentrations (mixed

ANOVA: $F_{(2, 12)} = 0.18$, $P = 0.840$, η^2 G = 0.02) or relative concentrations ($F_{(2, 12)} = 1.82$, $P = 0.200$, η^2 G = 0.17) (**Table S1**). However, DOC loss varied along the incubation period both for absolute ($F_{(1.19, 14.32)} = 127$, $P = 7.53 \times 10^{-9}$, η^2 G = 0.82) and relative concentrations ($F_{(1.39, 16.71)} = 290$, $P = 8.02 \times 10^{-13}$, η^2 G = 0.88) (**Fig. 3**). Mean DOC loss increased between day 29 (mean ± SE: 1.0 ± 0.3 mg L^{-1} or 7.1 ± 1.7%) and day 97 (5.0 ± 0.2 mg L^{-1} or 33.2 ± 1.1%), plateauing from day 97 until the end of the assay at day 188 (5.0 ± 0.3 mg L^{-1} or 33.4 ± 1.2%).

Under nutrient-replete incubations, DOC loss ranged between 0.1–8.5 mg L^{-1} (1–46% of initial DOC) across all samples and incubation times. DOC loss was not affected by nutrient addition, either in terms of absolute (mixed ANOVA: $F_{(2, 12)} = 0.100$, $P = 0.760$, η^2 G = 0.002) or relative concentrations ($F_{(2, 12)} = 0.183$, $P = 0.680$, η^2 G = 0.007) (**Table S1**). There was no detectable interaction effect between pond category and nutrient addition on absolute ($F_{(2, 12)} = 1.72$, $P = 0.220$, η^2 G = 0.06) and relative DOC loss ($F_{(2, 12)} = 1.63$, $P = 0.237$, η^2 G = 0.11).

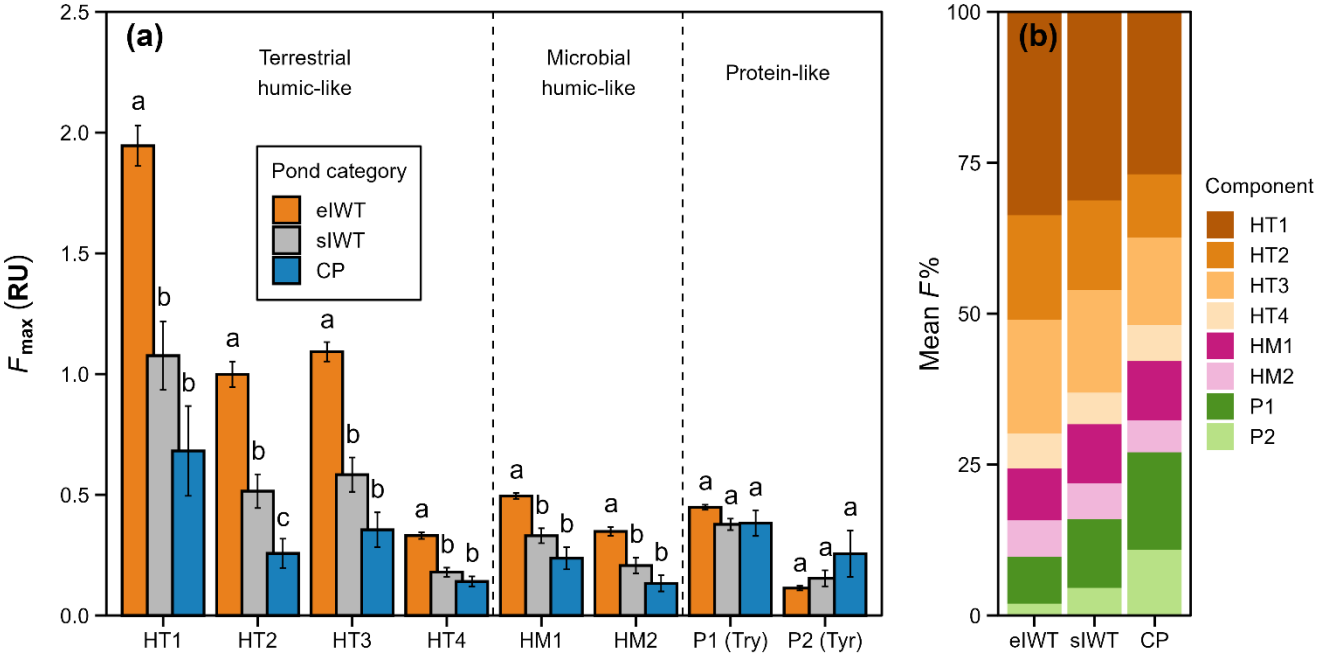

Figure 2: Absolute (a; mean ± SE, n = 5) and relative (b; mean) fluorescence intensity for the components identified by PARAFAC analysis at the beginning of the bioassay for each pond category. The components are divided to terrestrial humic-like (HT1–HT4), microbial humic-like (HM1 and HM2), and protein-like (tryptophan-like component P1 = Try, and tyrosine-like component P2 = Tyr) according to their fluorescence characteristics. For each component, different letters in panel (a) represent significant differences between pond categories as determined by Tukey HSD tests ($P < 0.05$).

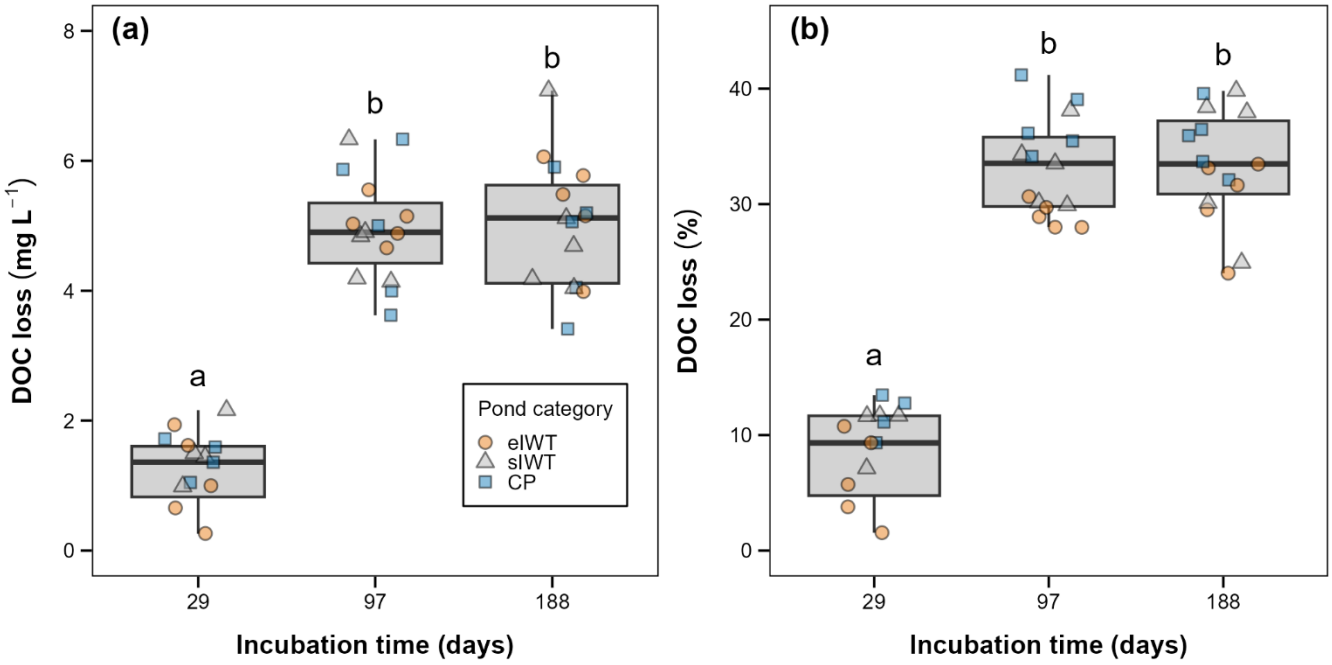

Figure 3: DOC loss during the 188-day dark bioassay using 2.7 µm-filtered pond water incubated at 15°C at ambient nutrient concentrations (n = 15). Results are expressed as DOC loss (a) and percentage DOC loss relative to initial DOC concentration (b). Boxplots indicate median (line), 1st and 3rd quartile (box margins), and 5 and 95% percentiles (whiskers). Different letters represent significant differences as determined by pairwise t-tests with Bonferroni correction ($P < 0.0001$).

3.3 Decay coefficients

The exponential decay model with a residual pool best described DOC decomposition during the bioassays, offering the optimal balance with respect to Akaike weights and RMSE (**Table S2**). However, since the plateau at the end of the decay curve is not supported by data points beyond 188 days, the estimated size of the residual DOC pool may be biased (e.g., **Fig. S2**). As a result, we focused our analysis on the decay coefficient (k), rather than on the residual DOC fraction. The distribution of decay coefficients obtained from the exponential model with residual pool closely matched the distribution of initial apparent decay coefficients from the reactivity continuum model (calculated as υ / a, in day^{-1}). In contrast, the decay coefficients derived from the simple exponential model were similar to those from the linear model, which showed the poorest performance among the models tested (**Fig. S3**).

First-order decay constants (k) ranged from 0.009 to 0.034 day^{-1} in unamended samples and from 0.011 to 0.063 day^{-1} in nutrient-replete samples (**Fig. 4**). Both pond category (F-tests for fixed effects: $F_{(2, 181)} = 20.1$, $P = 1.35 \times 10^{-8}$) and nutrient addition ($F_{(1, 181)} = 32.8$, $P = 4.25 \times 10^{-8}$) had significant effects on k. The interaction between the two factors indicated that the effect of nutrient addition on k depended on pond category ($F_{(2, 181)} = 137$, $P = 6.14 \times 10^{-24}$). However, pairwise comparisons revealed no significant differences between groups; the lowest P-value observed was 0.31 for the comparison between unamended eIWT and CP ponds (**Fig. 4**). Notably, the estimated means were associated with considerable uncertainty.

3.4 Drivers of DOM bioreactivity

Regression analysis revealed that the fluorescence intensity of the tryptophan-like component P1 was the strongest predictor of DOC loss on days 97 and 188 of the bioassay (**Fig. 5**, **Table S3**). Models using P1 intensity as the sole predictor had substantially higher Akaike weights (0.42 and 0.41 for days 97 and 188, respectively) than the next best models, which had weights of 0.19 and 0.14 at the same time points, but included Chl*a* alongside P1 as predictors (**Table S3**). Additionally, P1 was the only variable whose regression coefficient differed significantly from zero (based on t-tests) across all retained models. The decline in P1 fluorescence over time was also evident in EEMs collected at the beginning and end of the bioassay (**Fig. 6**). This result was consistent with the temporal dynamics of the individual PARAFAC components, showing a steady decrease in P1 fluorescence throughout the experiment (**Fig. S4**). Regression analysis also indicated that higher levels of CDOM were associated with lower decay coefficients (**Fig. 5**).

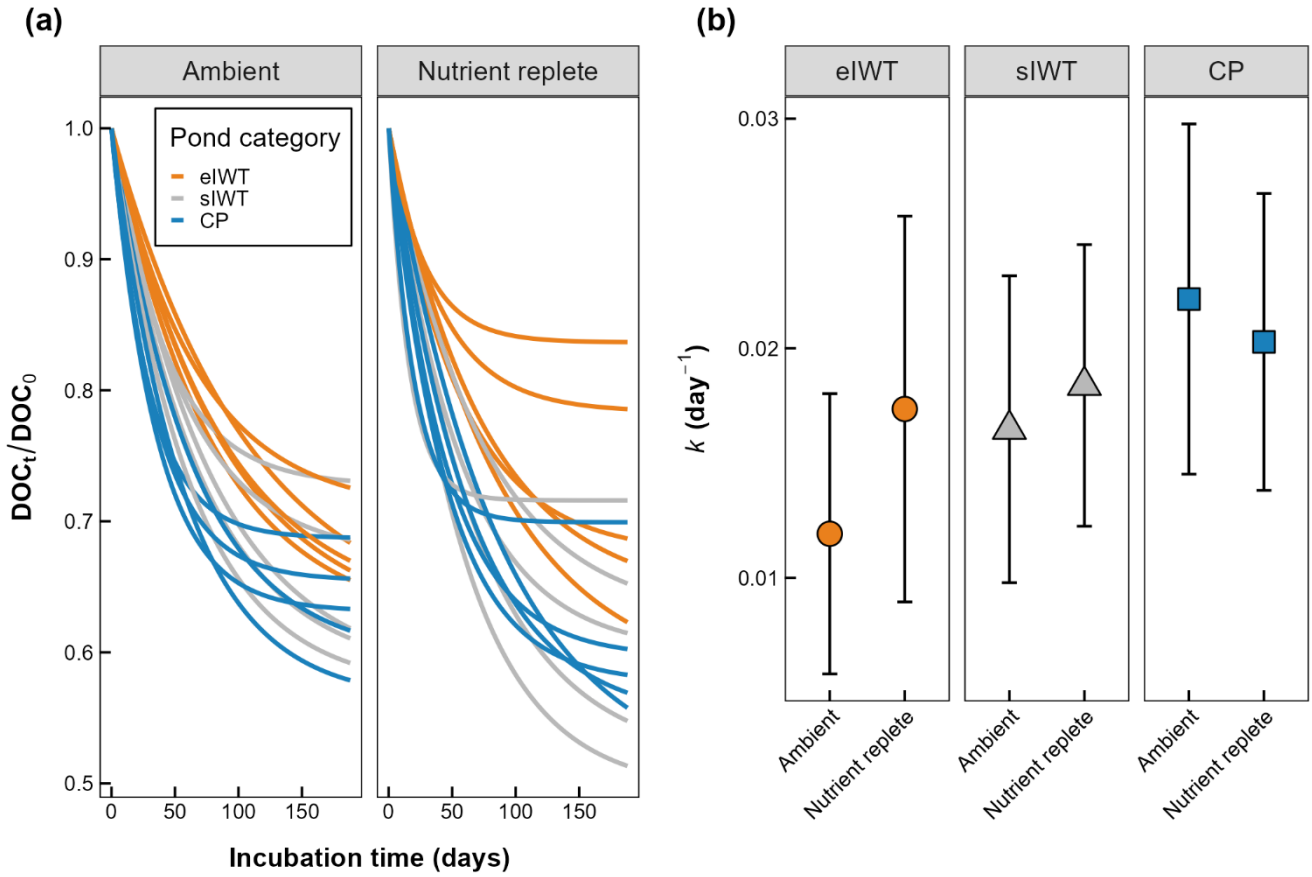

Figure 4: (a) exponential decay model with residual DOC pool fitted to the time series of relative DOC decomposition during the 188-day dark bioassay using 2.7 µm-filtered pond water incubated at 15°C, and (b) estimated decay coefficients and their 95% confidence intervals among the three pond categories (n = 5). The samples were incubated at ambient nutrient concentrations or amended with inorganic nitrogen and phosphorus (nutrient replete).

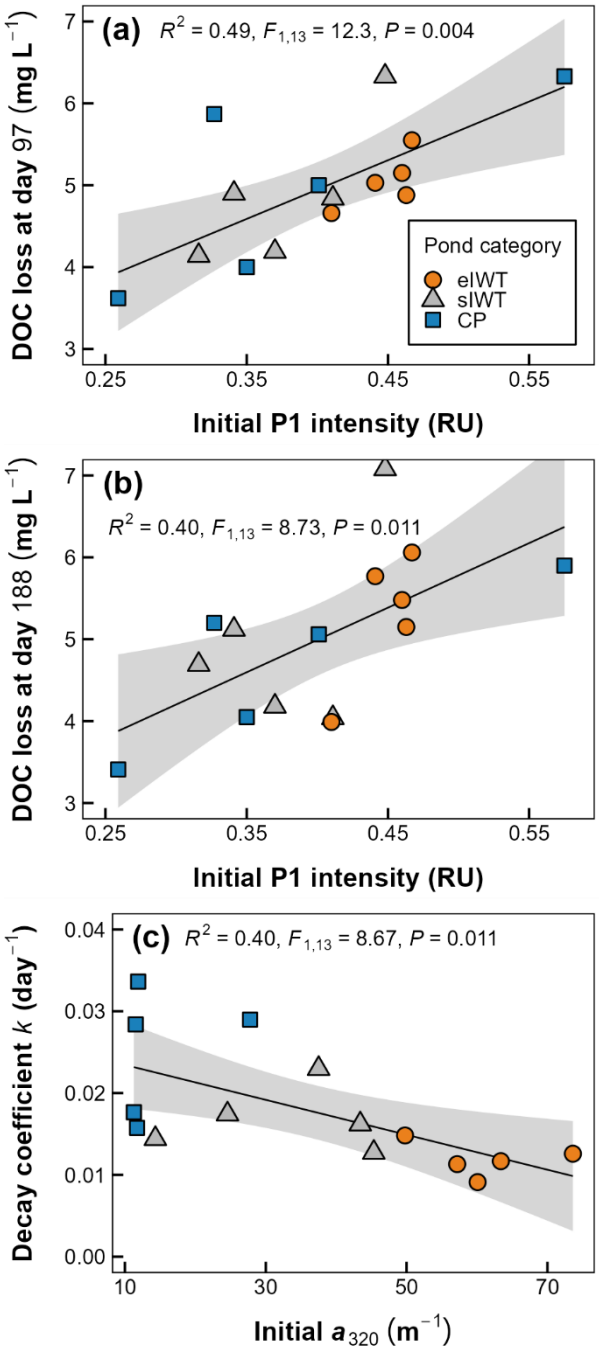

Figure 5: Relationships between the fluorescence intensity of the tryptophan-like fluorophore P1 identified by PARAFAC analysis and DOC loss at day 97 (a), or DOC loss at day 188 (b), and relationship between the absorption coefficient measured at 320 nm (a_{320}) and the DOC decay coefficient *k* (c).

4 Discussion

4.1 Extended microbial DOC decomposition in ice-wedge polygonal tundra ponds exceeds short-term estimates

Our results demonstrate substantial DOC decomposition by heterotrophic bacteria in the sampled ponds during the growing season, occurring on a timescale that exceed that of traditional bioassays. Most of the bioreactive DOC was processed after one month, with DOC losses exceeding 30% (or 5 mg L^{-1}) by day 97 of the bioassay, after which no further loss was observed (**Fig. 3**, **Table S1**). DOC bioavailability is typically assessed using standardized bioassays that measure DOC disappearance or CO_2 production over a period of days to weeks (McDowell et al., 2006; Vonk et al., 2015a). However, this timeframe is likely much shorter than the actual water residence time in the hydrologically isolated ponds of the polygonal tundra. Although water residence time was not estimated at the study site, previous studies have shown that hydrological connectivity in polygonal tundra ponds is reduced during summer: during this period, trough ponds receive subsurface water inflows from elevated low-center polygon ponds (not included in our study), while outflows are negligible, especially in ponds located on flat terrain and underlain by silty soils with low hydraulic conductivity (Helbig et al., 2013; Koch et al., 2014). Short-term bioassays may therefore substantially underestimate microbial DOC decomposition in Arctic ponds with limited summer runoff. In this regard, our findings are consistent with those of Vähätalo and Wetzel (2008), who showed that wetland-derived organic carbon can be degraded in surface waters given a sufficiently long residence time. They also reinforce the relevance of the concept of "hydrological biolability", introduced by Vonk et al. (2013), which emphasizes that the degradability of organic matter must be considered within the context of a system's water residence time. While short-term incubations (e.g., one month) remain useful for comparing DOM biolability across seasons or systems, they are likely to underestimate carbon loss when they do not reflect the duration of organic matter retention in aquatic environments.

DOC loss measured during the first month of incubation (1.0 ± 0.2 mg L^{-1} or 7.1 ± 1.7% by day 29) was nonetheless consistent with previous studies. Earlier field incubations in ponds within the same polygonal complex reported negligible DOC loss over a 12-day period (< 0.5 mg L^{-1}), under the combined influence of microbial decomposition and sunlight exposure (Laurion et al., 2021). In the latter study, water was collected following a particularly dry period, which likely limited the input of fresh DOM to the ponds. Our estimates over this timescale also fall within the range of bioavailable DOC reported for other aquatic systems in permafrost regions. For example, DOC loss in lakes, streams, and rivers across Alaska, Siberia, and western Canada has been reported to range between 3% and 18% within one month (Vonk et al., 2015a). Similarly, bioassays of comparable duration (28 days) conducted in waters from frozen peat bogs in Northern Europe and a thermo-erosion gully on the Tibetan Plateau (discontinuous permafrost) yielded DOC losses ranging from 0% to 10% (Liu et al., 2018; Shirokova et al., 2019). Collectively, these results suggest that the most bioreactive compounds (i.e., those mineralized over the first weeks or so) constitute a relatively small fraction of the total DOC pool in aquatic systems influenced by organic-rich permafrost, and that ponds within the ice-wedge polygonal landscapes of the eastern Canadian Arctic conform to this broader pattern.

Although higher than previous estimations made over shorter timescales for similar environments, DOC loss measured in the eIWT ponds of Bylot Island (mean of 33% after 97 days) was lower than values reported for thermokarst aquatic systems

underlain by Pleistocene-age loess deposits, commonly referred to as Yedoma. Experimental thawing of Yedoma has shown that a large portion of its DOC pool (~50%) can be rapidly utilized by bacteria in soil pore water (Drake et al., 2015). Supporting the view of a highly labile Yedoma carbon pool, DOC bioavailability measured within 40 days is generally higher in thaw streams and outflows (12–62%) compared with undisturbed reference sites or main river stem (6–17%) (Abbott et al., 2014; Mann et al., 2015; Spencer et al., 2015; Vonk et al., 2013). Although DOM bioavailability varies along the soil-water continuum and is influenced by pre-sampling conditions (e.g., rainfall) and incubation methods (Abnizova et al., 2014; Vonk et al., 2015a), these studies collectively demonstrate that DOM is generally more reactive in aquatic landscapes underlain by Yedoma than in other organic-rich permafrost settings. The high bioreactivity of Yedoma-derived DOM has been attributed to its molecular composition, notably the abundance of saturated aliphatic compounds such as lipids, proteins, and carbohydrates (Spencer et al., 2015; Textor et al., 2019). A study by MacDonald et al. (2021) comparing several permafrost-derived DOM sources in the western Canadian Arctic (including tills, diamicton, lacustrine deposits, peat, and Yedoma) found that peat and Yedoma leachates had similar proportions of aliphatic compounds and aromaticity, suggesting comparable biodegradability potentials. The lower reactivity of DOM observed in the eIWT ponds of our study may therefore reflect differences in the molecular composition of DOM leached from permafrost, influenced by the nature of the parent material—on Bylot Island, a mix of peaty soils with sand and silts—and by transformation processes occurring before freezing or after thawing (MacDonald et al., 2021; Tank et al., 2020). A more detailed characterization of DOM using ultrahigh-resolution mass spectrometry (e.g., Spencer et al., 2015; Textor et al., 2019; Wologo et al., 2021) would provide valuable insights into its oxidation state and the relative proportions of aromatic versus aliphatic compounds in Bylot Island ponds, enabling direct comparisons with aquatic systems across regions with differing permafrost histories.

In our experiment, pond water was incubated at 15°C to standardize comparisons across pond categories and nutrient treatments (ambient versus nutrient-replete conditions). Given an *in situ* mean surface temperature of 10°C in July, microbial activity in the field over this period would likely be lower than that observed in our bioassays. Assuming a temperature coefficient (Q_{10}) of 2 (Wickland et al., 2012), the 33% loss of DOC observed after 97 days at 15°C would correspond to approximately 23% at 10°C. This 5°C discrepancy suggests that our lab-based incubations may overestimate DOC loss by approximately 30%. However, ponds are shallow and contain high levels of CDOM; thus, their surface waters can warm significantly during the day, with field measurements showing peak temperatures of 19°C in eIWT ponds in July 2017. This highlights the need for cautious interpretation of DOC loss and decay rates when accounting for natural thermal fluctuations. The temperature effect would need to be tested independently to fully resolve this question.

4.2 Comparable DOC loss measured despite varying levels of permafrost erosion

Contrary to our initial hypothesis, we observed comparable levels of DOC loss across pond categories, despite notable differences in DOC and TP concentrations and optical properties at the start of the bioassay (**Table 1** and **Fig. 2**). This finding was unexpected, yet it aligns with previous studies showing that DOM reactivity or dissolved CO_2 concentrations in surface waters are not consistently influenced by thermokarst activity (Heslop et al., 2021; Larouche et al., 2015). Two hypotheses

may explain the similar DOC loss observed across pond categories in our study: (i) planktonic bacteria rely primarily on a common DOM pool across pond categories, or (ii) differences in DOM composition result in similar overall losses due to microbial community adaptation to distinct organic matter sources (Crump et al., 2003; Marschner and Kalbitz, 2003). In support of hypothesis (i), it is possible that the majority of bioavailable DOM originates from a shared pool, which is produced *in situ* or by an external source, or modified by environmental factors such as sunlight exposure in the water column. This warrants more detailed assessments of DOM molecular composition and bacterial community structure.

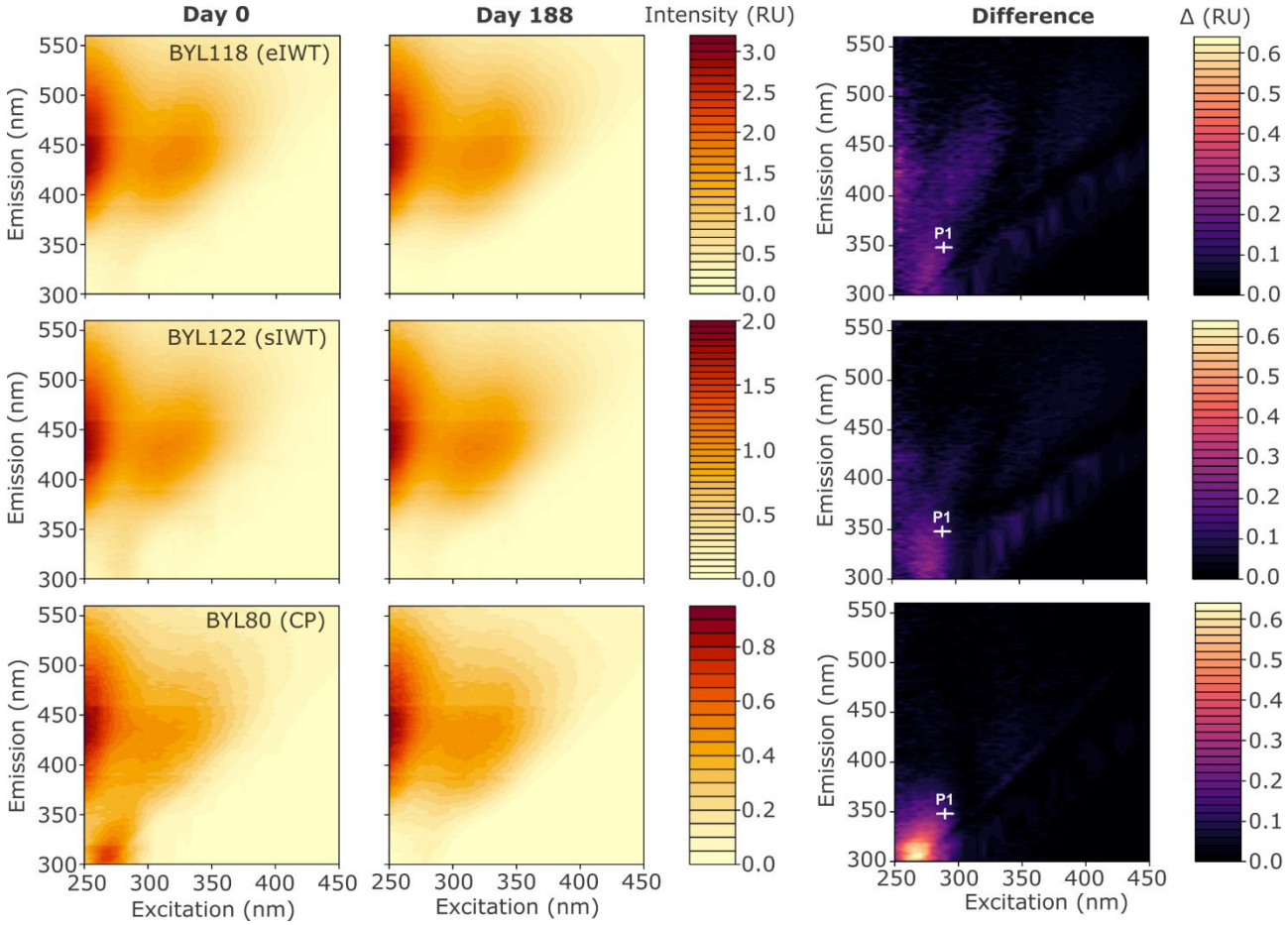

Figure 6: Representative fluorescence excitation-emission matrices (EEMs) for erosive ice-wedge trough (eIWT) ponds (top row), stable ice-wedge trough (sIWT) ponds (middle row), and coalescent polygon (CP) ponds (bottom row) at the start (left column) and end (day 188; middle column) of the bioassay. The right column shows the difference in fluorescence intensity between the two time points, with markers indicating the P1 peak excitation-emission maxima. Note the differences in fluorescence intensity scales for the EEMs at t_0 (left column) and t_{188} (middle column) across ponds.

4.3 No effect of nutrient addition on DOC turnover rate

Nutrient amendment in our bioassay had little or no impact on DOC loss or decomposition dynamics under the conditions tested (**Fig. 4**). Consistently, neither initial TP nor TN concentrations were identified as significant predictors of DOC loss in regression analyses: each was included in only one model, with non-significant coefficients (**Table S3**). These findings support our initial hypothesis that N and P availability in these waterbodies exceeds the amount required for decomposition relative to the available DOC pool (Pacoureau et al., 2025). Previous studies examining the effects of nutrient addition on DOM bioreactivity in permafrost regions have produced mixed results. Negative effects on DOC mineralization were reported in streams from Canada, interior Alaska, and the Tibetan Plateau (Wologo et al., 2021), while positive effects were observed during spring freshet in Alaskan rivers and streams (Holmes et al., 2008; Mutschlecner et al., 2018). In thermokarst-impacted outflows on the North Slope of Alaska, Abbott et al. (2014) found no effect of inorganic N and P addition on BDOC measured over 40 days, but observed a twofold increase in decomposed DOC after 10 days of incubation (17.5% on average, compared with 9.2% in the unamended control). They also found that sites with the highest baseline dissolved inorganic nitrogen concentrations exhibited the strongest response to inorganic nutrient enrichment. These contrasting outcomes likely reflect variability in background nutrient availability across surface waters in permafrost regions, suggesting that carbon cycling responses to nutrient inputs are highly context-dependant. However, inconsistent reporting of nutrient concentrations across studies limits our ability to relate bacterial DOM-degradation responses to specific stoichiometric thresholds.

In our study, while nutrient addition appeared to enhance DOC decomposition rates in eIWT ponds (**Fig. 4**), stoichiometric analyses revealed that eIWT ponds showed the highest DOC:TN ratios (**Table 1**), suggesting that nitrogen limitation of bacterial DOC decomposition was most likely in these thermokarst ponds. This hypothesis is supported by the inclusion of TN as a predictor in the second-best model explaining variation in the decay coefficient *k* (**Table S3**), although this variable was not significant. However, firm conclusions regarding the link between nitrogen availability and DOC decomposition rates cannot be drawn without experimental manipulation of nitrogen alone (i.e., inorganic N addition without phosphorus), and a larger sample size to increase the statistical power of the test.

The nutrient concentrations used in our bioassay do not reflect any known scenario of nutrient enrichment in permafrost-affected surface waters, and were designed to test whether added N and P could alleviate limitation of bacterial DOC decomposition. Previous work has shown that permafrost thaw may increase N and P delivery to Arctic surface waters via runoff or drainage, as large nutrient stores are mobilized (Vonk et al., 2015b). However, in organic-rich tundra ponds such as those on Bylot Island, DOC decomposition and turnover appear largely unresponsive to nutrient enrichment. These systems already have relatively high concentrations of N and P and exhibit low DOC:TN and DOC:TP molar ratios (**Table 1**, see also Pacoureau et al., 2025), suggesting that DOM composition—rather than nutrient availability—may be the primary constraint on microbial degradation.

4.4 Protein-like FDOM as an indicator of DOM bioreactivity

The positive linear relationship between initial fluorescence intensity of the tryptophan-like component P1 and DOC loss (**Fig. 5**) suggests that P1 represents a significant fraction of the bioreactive DOM pool in the studied tundra ponds. This result aligns with previous research in freshwater systems and soil pore waters, where protein-like FDOM has been correlated with DOM bioreactivity and shown to be preferentially removed relative to humic-like compounds (Balcarczyk et al., 2009; Baradaran et al., 2025; Fellman et al., 2008). The similar P1 fluorescence intensities across pond categories (**Fig. 2**) may also indicate rapid cycling of these compounds in the studied systems (i.e., fast turnover rates). The protein-like FDOM in the ponds was previously associated with small-sized organic molecules, likely derived from aquatic and terrestrial vegetation or from cyanobacterial benthic mats (Pacoureau et al., 2025). Allain et al. (2023) showed that leachates from vegetation collected in subarctic environments were dominated by tyrosine- and tryptophan-like fluorophores, suggesting high biolability due to the presence of lipids, amino acids, proteins, and carbohydrates. Similarly, Textor et al. (2019) reported high microbial utilization (> 60% over 28 days) of DOC in plant leachates from the Yukon Basin in Alaska. Taken together, these findings suggest that terrestrial plants and aquatic vegetation may be key precursors of biolabile DOM in tundra ponds. Their role in supporting microbial activity warrants further investigation, especially in the context of Arctic greening (Fraser et al., 2011; Ju and Masek 2016). This trend may enhance the input of bioreactive, protein-like DOM typically associated with autochthonous production. The bioreactive protein-like FDOM fraction consumed by bacteria during incubations could also originate from phytoplankton and microphytobenthos biomass living or decomposing within the ponds. In this regard, it is noteworthy that Chl*a* was selected as a potential predictor of DOC loss in the second-best regression models (**Table S3**). As indicated by Chl*a* concentrations (**Table 1**), these warm, shallow, and nutrient-rich water bodies are productive systems in the tundra, especially compared with the oligotrophic lakes present in the catchment. Phytoplankton likely influence carbon cycling, notably by enhancing atmospheric CO_2 uptake and contributing inputs of recently fixed carbon. However, phytobenthic biomass often exceeds phytoplanktonic biomass in northern lakes and ponds where sufficient light can reach the bottom, thus accounting for most of the autotrophic productivity (Jeppesen et al., 2021). It is possible that these phototrophic colonies established in sIWT and CP ponds release organic compounds into the water, thereby enhancing DOC decay at the onset of incubations relative to eIWT ponds (**Fig. 4**). Because incubations were done in the dark, these primary producers would not have continued to release labile compounds over the experimental period.

4.5 Fate of the remaining DOC pool

The open-water season for ponds at this latitude lasts only about 90 days (Prėskienis et al., 2021), followed by complete freeze-up. Given that 59–72% of the DOC remained undegraded after ~100 days of dark incubation (**Fig. 3**), except for the fraction mineralized under the action of sunlight (Cory and Kling, 2018), a certain portion of this pool may ultimately be converted into particulate organic carbon (POC) through cryoconcentration and colloid coagulation (Manasypov et al., 2015). Therefore, semi-labile organic matter could accumulate in anoxic pond sediments, potentially contributing to long-term pond infilling, as

previously suggested for ponds in polygonal terrains (Koch et al., 2018). Part of this POC and the remaining colloidal material may become available to bacteria again during the open-water season via resuspension during periods of water column mixing. Repeated freeze-thaw cycles have been shown to cause mechanical degradation of organic and organo-mineral colloids in circumneutral ponds and lakes in permafrost regions, potentially increasing DOM reactivity by generating low molecular weight compounds and removing aromatic carbon (Pokrovsky et al., 2018). Further research is needed to better understand the effect of freeze-thaw cycles on DOC dynamics in polygonal tundra ponds.

4.6 Snapshot of bacterial DOC decomposition during summer

Although the ice-free season is brief at our field site, we captured only a snapshot of biogeochemical conditions and DOM decomposition potential during summer. The outcome may differ following rainfall events or during extended dry periods. Moreover, the snowmelt period, previously identified as a critical time for DOM input in tundra ponds (Fouché et al., 2017), may involve DOM with different composition and reactivity. Beyond microbial degradation, several processes contribute to the removal of organic matter in aquatic systems. These include partial or complete photo-oxidation, which breaks down organic molecules into smaller compounds or CO_2 (Wetzel et al., 1995); flocculation, which aggregates DOM into particulate form (von Wachenfeldt and Tranvik, 2008); and sorption to mineral particles (Marschner and Kalbitz, 2003). Photodegradation has received increasing attention in northern inland waters due to its role in CDOM bleaching and its contribution to CO_2 emissions (Bertilsson and Tranvik, 2000; Del Vecchio and Blough, 2002; Koehler et al., 2014). In addition, UV radiation exposure has been shown to stimulate microbial DOM utilization in thermokarst-impacted aquatic systems (Cory et al., 2013; Mazoyer et al., 2022). Although evidence remains insufficient to fully characterize all mechanisms involved, sunlight-induced changes in DOM composition may promote shifts in bacterial community structure and activity (Judd et al., 2007; Ward et al., 2017). In our bioassay, the high contribution of chromophoric, humic-like molecules to the fluorescent DOM pool (**Fig. 2**) suggests that exposure to sunlight would likely have resulted in additional DOC losses, thereby amplifying the potential for carbon release to the atmosphere. Regarding flocculation, we observed flocs in three incubation bottles but could not quantify the associated DOC loss because of limited sample volume. Although flocculation during incubation or after acidification for DOC preservation could overestimate DOC attributed to microbial degradation, DOC loss patterns were consistent across all samples, and the three affected bottles did not systematically deviate from these trends. This suggest that flocculation in these cases (and likely overall) did not substantially bias our conclusions about DOC bioavailability among pond categories. Nonetheless, additional processes such as photodegradation, flocculation, and sorption to mineral particles should be explicitly addressed in future work, as they may influence DOM fate under conditions different from those applied in the present study. In our incubations, initial CDOM (a_{320}) levels in the ponds were negatively correlated with the DOC decay coefficient k (**Fig. 5**). Although statistically non-significant, we also observed a trend in which k increased from eIWT to CP ponds (**Fig. 4**), consistent with increasing average CDOM levels across these systems. Similar negative relationships between CDOM and decay coefficients have been shown for lacustrine environments (Koehler et al., 2012). CDOM is widely used as a proxy for terrestrial DOM contributions in aquatic systems. In the organic-rich ponds of the polygonal tundra, the concurrent decrease

in *k* despite increasing CDOM concentrations suggests that permafrost-derived DOM inputs are poorly available for bacterial communities under the dark incubation conditions tested here.

This study primarily aimed to elucidate variation in DOM bioreactivity across geomorphologically distinct pond systems and identify key compositional drivers of decomposition processes. While not intended to generate global carbon cycle quantifications, our mechanistic findings provide critical insights into small-waterbody biogeochemistry that may inform future synthesis efforts.

5 Conclusion

To our knowledge, this study provides the first estimates of microbial DOM decomposition in ponds within ice-wedge polygonal landscapes using bioassays lasting longer than one month. The patterns of DOM decomposition observed in our study provide important insights into the factors influencing DOM transformation in tundra ponds affected by permafrost degradation. Our results suggest that during the relatively short ice-free period, dark heterotrophic processes in the water column can alone transform approximately one third of the DOM pool. Given the substantial DOC loss observed here, the predicted lengthening of the growing season in the Arctic, and the expanding surface area of small waterbodies driven by permafrost thaw and erosion, microbial DOM decomposition is likely to increasingly contribute to CO_2 production in polygonal tundra ponds on Holocene peat-silt deposits. However, this contribution may remain below that of comparable waterbodies on Yedoma, due to lower DOM concentrations and bioreactivity. We showed that the protein-like FDOM fraction was linked to the concentration of bioreactive organic matter in these systems, supporting the idea that DOM composition strongly influences its lability in Arctic freshwaters. Future work should determine whether this fraction originates from contemporary DOM (i.e., vegetation or algal production) or from aged permafrost DOM, to better assess the contribution of water column microbial processes to the permafrost carbon feedback. Finally, thermokarst-driven nutrient export may have only a limited effect on DOC turnover in organic-rich thaw ponds. However, this hypothesis requires testing across a broader range of permafrost aquatic systems, with consistent reporting of N and P concentrations to assess under which conditions bacterial DOM decomposition may be affected. As spatial datasets expand and process-based models advance in resolving fine-scale aquatic ecosystems, these results could contribute to more robust predictions of carbon processing in heterogeneous pond landscapes.

Data availability

All data supporting the findings of this study are available in the Borealis repository at the following address: https://doi.org/10.5683/SP3/WO5DUT.

Author contribution

Thomas Pacoureau: conceptualization (equal), data curation (lead), formal analysis (lead), investigation (lead), methodology (lead), resources (equal), software (lead), validation (lead), visualization (lead), writing – original draft preparation (lead), writing – review & editing (equal). Isabelle Laurion: conceptualization (equal), founding acquisition (lead), investigation (supporting), methodology (supporting), project administration (lead), resources (supporting), supervision (lead), writing – review & editing (equal). Milla Rautio: conceptualization (equal), founding acquisition (supporting), writing – review & editing (equal).

Competing interests

The authors declare that they have no conflict of interest.

Acknowledgments

We gratefully thank F. Mazoyer for field and laboratory assistance, D. Bélanger, J. Perreault and L. Rancourt for water chemistry analysis, and F. Soulat for flux cytometry analysis. We also express our gratitude to J. Comte for providing a valuable insight on bacterial enumeration. This research was supported by the Natural sciences and engineering research council of Canada (Discovery and Northern Supplement grants to IL, and CREATE EnviroNorth scholarship to TP), and the Polar Continental Shelf Program (Natural Resources Canada). We acknowledge the Center for Northern Studies (CEN) for access to the research infrastructures, Parks Canada and the community of Mittimatalik for granting access to the study site, and the Interuniversity Research Group in Limnology (GRIL) for providing access to their analytical services. This work was carried out in the traditional territories of the Inuit, Nunangat.

References

Abbott, B. W., Larouche, J. R., Jones Jr., J. B., Bowden, W. B., and Balser, A. W.: Elevated dissolved organic carbon biodegradability from thawing and collapsing permafrost, Journal of Geophysical Research: Biogeosciences, 119, 2049–2063, https://doi.org/10.1002/2014JG002678, 2014.

Abbott, B. W., Jones, J. B., Godsey, S. E., Larouche, J. R., and Bowden, W. B.: Patterns and persistence of hydrologic carbon and nutrient export from collapsing upland permafrost, Biogeosciences, 12, 3725–3740, https://doi.org/10.5194/bg-12-3725-2015, 2015.

Abnizova, A., Young, K. L., and Lafrenière, M. J.: Pond hydrology and dissolved carbon dynamics at Polar Bear Pass wetland, Bathurst Island, Nunavut, Canada, Ecohydrology, 7, 73–90, https://doi.org/10.1002/eco.1323, 2014.

Allain, A., Alexis, M. A., Bridoux, M. C., Humbert, G., Agnan, Y., and Rouelle, M.: Fingerprinting the elemental composition and chemodiversity of vegetation leachates: consequences for dissolved organic matter dynamics in Arctic environments, Biogeochemistry, 164, 73–98, https://doi.org/10.1007/s10533-022-00925-9, 2023.

Allard, M., Sarrazin, D., and l'Hérault, E.: Borehole and near-surface ground temperatures in northeastern Canada (1.6.0 (1988-2023)), https://doi.org/10.5885/45291SL-34F28A9491014AFD, 2024.

Allesson, L., Andersen, T., Dörsch, P., Eiler, A., Wei, J., and Hessen, D. O.: Phosphorus Availability Promotes Bacterial DOC-Mineralization, but Not Cumulative CO2-Production, Front. Microbiol., 11, https://doi.org/10.3389/fmicb.2020.569879, 2020.

Ateia, M., Ran, J., Fujii, M., and Yoshimura, C.: The relationship between molecular composition and fluorescence properties of humic substances, Int. J. Environ. Sci. Technol., 14, 867–880, https://doi.org/10.1007/s13762-016-1214-x, 2017.

Balcarczyk, K. L., Jones, J. B., Jaffé, R., and Maie, N.: Stream dissolved organic matter bioavailability and composition in watersheds underlain with discontinuous permafrost, Biogeochemistry, 94, 255–270, https://doi.org/10.1007/s10533-009-9324-x, 2009.

Baradaran, S. C., Guillemette, F., and Lapierre, J.-F.: Abrupt shifts in the concentration, composition, and reactivity of dissolved organic carbon from terrestrial to aquatic compartments across boreal watersheds, Sci Rep, 15, 21387, https://doi.org/10.1038/s41598-025-06877-y, 2025.

Bartoń, K.: _MuMIn: Multi-Model Inference_, 2024.

Berggren, M., Laudon, H., Jonsson, A., and Jansson, M.: Nutrient Constraints on Metabolism Affect the Temperature Regulation of Aquatic Bacterial Growth Efficiency, Microb Ecol, 60, 894–902, https://doi.org/10.1007/s00248-010-9751-1, 2010.

Berggren, M., Gudasz, C., Guillemette, F., Hensgens, G., Ye, L., and Karlsson, J.: Systematic microbial production of optically active dissolved organic matter in subarctic lake water, Limnology and Oceanography, 65, 951–961, https://doi.org/10.1002/lno.11362, 2020.

Berggren, M., Ye, L., Sponseller, R. A., Bergström, A.-K., Karlsson, J., Verheijen, H., and Hensgens, G.: Nutrient limitation masks the dissolved organic matter composition effects on bacterial metabolism in unproductive freshwaters, Limnology and Oceanography, 68, 2059–2069, https://doi.org/10.1002/lno.12406, 2023.

Bertilsson, S. and Tranvik, L. J.: Photochemical transformation of dissolved organic matter in lakes, Limnology and Oceanography, 45, 753–762, https://doi.org/10.4319/lo.2000.45.4.0753, 2000.

Bilodeau, F., Gauthier, G., and Berteaux, D.: The effect of snow cover on lemming population cycles in the Canadian High Arctic, Oecologia, 172, 1007–1016, https://doi.org/10.1007/s00442-012-2549-8, 2013.

Breton, J., Vallières, C., and Laurion, I.: Limnological properties of permafrost thaw ponds in northeastern Canada, Can. J. Fish. Aquat. Sci., 66, 1635–1648, https://doi.org/10.1139/F09-108, 2009.

CEN: Climate station data from Bylot Island in Nunavut, Canada (1.11 (1992-2019)), https://doi.org/10.5885/45039SL-EE76C1BDAADC4890, 2020.

Cory, R. M. and Kling, G. W.: Interactions between sunlight and microorganisms influence dissolved organic matter degradation along the aquatic continuum, Limnology and Oceanography Letters, 3, 102–116, https://doi.org/10.1002/lol2.10060, 2018.

Cory, R. M., Crump, B. C., Dobkowski, J. A., and Kling, G. W.: Surface exposure to sunlight stimulates CO2 release from permafrost soil carbon in the Arctic, Proceedings of the National Academy of Sciences, 110, 3429–3434, https://doi.org/10.1073/pnas.1214104110, 2013.

Crump, B. C., Kling, G. W., Bahr, M., and Hobbie, J. E.: Bacterioplankton Community Shifts in an Arctic Lake Correlate with Seasonal Changes in Organic Matter Source, Applied and Environmental Microbiology, 69, 2253–2268, https://doi.org/10.1128/AEM.69.4.2253-2268.2003, 2003.

Dean, J. F., van Hal, J. R., Dolman, A. J., Aerts, R., and Weedon, J. T.: Filtration artefacts in bacterial community composition can affect the outcome of dissolved organic matter biolability assays, Biogeosciences, 15, 7141–7154, https://doi.org/10.5194/bg-15-7141-2018, 2018.

Del Vecchio, R. and Blough, N. V.: Photobleaching of chromophoric dissolved organic matter in natural waters: kinetics and modeling, Marine Chemistry, 78, 231–253, https://doi.org/10.1016/S0304-4203(02)00036-1, 2002.

Deshpande, B. N., Crevecoeur, S., Matveev, A., and Vincent, W. F.: Bacterial production in subarctic peatland lakes enriched by thawing permafrost, Biogeosciences, 13, 4411–4427, https://doi.org/10.5194/bg-13-4411-2016, 2016.

Drake, T. W., Wickland, K. P., Spencer, R. G. M., McKnight, D. M., and Striegl, R. G.: Ancient low–molecular-weight organic acids in permafrost fuel rapid carbon dioxide production upon thaw, Proceedings of the National Academy of Sciences, 112, 13946–13951, https://doi.org/10.1073/pnas.1511705112, 2015.

Fellman, J. B., D'Amore, D. V., Hood, E., and Boone, R. D.: Fluorescence characteristics and biodegradability of dissolved organic matter in forest and wetland soils from coastal temperate watersheds in southeast Alaska, Biogeochemistry, 88, 169–184, https://doi.org/10.1007/s10533-008-9203-x, 2008.

Fouché, J., Lafrenière, M. J., Rutherford, K., and Lamoureux, S.: Seasonal hydrology and permafrost disturbance impacts on dissolved organic matter composition in High Arctic headwater catchments, Arctic Science, 3, 378–405, https://doi.org/10.1139/as-2016-0031, 2017.

Fouché, J., Christiansen, C. T., Lafrenière, M. J., Grogan, P., and Lamoureux, S. F.: Canadian permafrost stores large pools of ammonium and optically distinct dissolved organic matter, Nat Commun, 11, 4500, https://doi.org/10.1038/s41467-020-18331-w, 2020.

Fraser, R. H., Olthof, I., Carrière, M., Deschamps, A., and Pouliot, D.: Detecting long-term changes to vegetation in northern Canada using the Landsat satellite image archive, Environ. Res. Lett., 6, 045502, https://doi.org/10.1088/1748-9326/6/4/045502, 2011.

Granéli, W., Bertilsson, S., and Philibert, A.: Phosphorus limitation of bacterial growth in high Arctic lakes and ponds, Aquat. Sci., 66, 430–439, https://doi.org/10.1007/s00027-004-0732-7, 2004.

Guillemette, F. and del Giorgio, P. A.: Simultaneous consumption and production of fluorescent dissolved organic matter by lake bacterioplankton, Environmental Microbiology, 14, 1432–1443, https://doi.org/10.1111/j.1462-2920.2012.02728.x, 2012.

Helbig, M., Boike, J., Langer, M., Schreiber, P., Runkle, B. R. K., and Kutzbach, L.: Spatial and seasonal variability of polygonal tundra water balance: Lena River Delta, northern Siberia (Russia), Hydrogeol J, 21, 133–147, https://doi.org/10.1007/s10040-012-0933-4, 2013.

Helms, J. R., Stubbins, A., Ritchie, J. D., Minor, E. C., Kieber, D. J., and Mopper, K.: Absorption spectral slopes and slope ratios as indicators of molecular weight, source, and photobleaching of chromophoric dissolved organic matter, Limnology and Oceanography, 53, 955–969, https://doi.org/10.4319/lo.2008.53.3.0955, 2008.

Heslop, J. K., Hung, J. K. Y., Tong, H., Simpson, M. J., Chapman, F. M., Roulet, N., Lafrenière, M. J., and Lamoureux, S. F.: Diverging pond dissolved organic matter characteristics yield similar CO2 flux potentials in a disturbed High Arctic landscape, Environ. Res. Lett., 16, 044016, https://doi.org/10.1088/1748-9326/abc913, 2021.

Holmes, R. M., McClelland, J. W., Raymond, P. A., Frazer, B. B., Peterson, B. J., and Stieglitz, M.: Lability of DOC transported by Alaskan rivers to the Arctic Ocean, Geophysical Research Letters, 35, https://doi.org/10.1029/2007GL032837, 2008.

Jeppesen, E., Christoffersen, K. S., Rautio, M., and Lauridsen, T. L.: Ecology of Arctic Lakes and Ponds, in: Arctic Ecology, John Wiley & Sons, Ltd, 159–180, https://doi.org/10.1002/9781118846582.ch7, 2021.

Ju, J. and Masek, J. G.: The vegetation greenness trend in Canada and US Alaska from 1984–2012 Landsat data, Remote Sensing of Environment, 176, 1–16, https://doi.org/10.1016/j.rse.2016.01.001, 2016.

Judd, K. E., Crump, B. C., and Kling, G. W.: Bacterial responses in activity and community composition to photo-oxidation of dissolved organic matter from soil and surface waters, Aquat. Sci., 69, 96–107, https://doi.org/10.1007/s00027-006-0908-4, 2007.

Karlsson, J., Serikova, S., Vorobyev, S. N., Rocher-Ros, G., Denfeld, B., and Pokrovsky, O. S.: Carbon emission from Western Siberian inland waters, Nat Commun, 12, 825, https://doi.org/10.1038/s41467-021-21054-1, 2021.

Kassambara, A.: rstatix: Pipe-Friendly Framework for Basic Statistical Tests, 2023.

Koch, J. C., Gurney, K., and Wipfli, M. S.: Morphology-Dependent Water Budgets and Nutrient Fluxes in Arctic Thaw Ponds, Permafrost and Periglacial Processes, 25, 79–93, https://doi.org/10.1002/ppp.1804, 2014.

Koch, J. C., Jorgenson, M. T., Wickland, K. P., Kanevskiy, M., and Striegl, R.: Ice Wedge Degradation and Stabilization Impact Water Budgets and Nutrient Cycling in Arctic Trough Ponds, Journal of Geophysical Research: Biogeosciences, 123, 2604–2616, https://doi.org/10.1029/2018JG004528, 2018.

Koehler, B., von Wachenfeldt, E., Kothawala, D., and Tranvik, L. J.: Reactivity continuum of dissolved organic carbon decomposition in lake water, Journal of Geophysical Research: Biogeosciences, 117, https://doi.org/10.1029/2011JG001793, 2012.

Koehler, B., Landelius, T., Weyhenmeyer, G. A., Machida, N., and Tranvik, L. J.: Sunlight-induced carbon dioxide emissions from inland waters, Global Biogeochemical Cycles, 28, 696–711, https://doi.org/10.1002/2014GB004850, 2014.

Lapierre, J.-F. and del Giorgio, P. A.: Partial coupling and differential regulation of biologically and photochemically labile dissolved organic carbon across boreal aquatic networks, Biogeosciences, 11, 5969–5985, https://doi.org/10.5194/bg-11-5969-2014, 2014.

Larouche, J. R., Abbott, B. W., Bowden, W. B., and Jones, J. B.: The role of watershed characteristics, permafrost thaw, and wildfire on dissolved organic carbon biodegradability and water chemistry in Arctic headwater streams, Biogeosciences, 12, 4221–4233, https://doi.org/10.5194/bg-12-4221-2015, 2015.

Laurion, I., Massicotte, P., Mazoyer, F., Negandhi, K., and Mladenov, N.: Weak mineralization despite strong processing of dissolved organic matter in Eastern Arctic tundra ponds, Limnology and Oceanography, 66, S47–S63, https://doi.org/10.1002/lno.11634, 2021.

Lenth, R. V., Piaskowski, J., Banfai, B., Bolker, B., Buerkner, P., Giné-Vázquez, I., Hervé, M., Jung, M., Love, J., Miguez, F., Riebl, H., and Singmann, H.: emmeans: Estimated Marginal Means, aka Least-Squares Means, 2025.

Liljedahl, A. K., Boike, J., Daanen, R. P., Fedorov, A. N., Frost, G. V., Grosse, G., Hinzman, L. D., Iijma, Y., Jorgenson, J. C., Matveyeva, N., Necsoiu, M., Raynolds, M. K., Romanovsky, V. E., Schulla, J., Tape, K. D., Walker, D. A., Wilson, C. J., Yabuki, H., and Zona, D.: Pan-Arctic ice-wedge degradation in warming permafrost and its influence on tundra hydrology, Nature Geosci, 9, 312–318, https://doi.org/10.1038/ngeo2674, 2016.

Liu, F., Chen, L., Zhang, B., Wang, G., Qin, S., and Yang, Y.: Ultraviolet radiation rather than inorganic nitrogen increases dissolved organic carbon biodegradability in a typical thermo-erosion gully on the Tibetan Plateau, Science of The Total Environment, 627, 1276–1284, https://doi.org/10.1016/j.scitotenv.2018.01.275, 2018.

Lougheed, V. L., Tweedie, C. E., Andresen, C. G., Armendariz, A. M., Escarzaga, S. M., and Tarin, G.: Patterns and Drivers of Carbon Dioxide Concentrations in Aquatic Ecosystems of the Arctic Coastal Tundra, Global Biogeochemical Cycles, 34, e2020GB006552, https://doi.org/10.1029/2020GB006552, 2020.

Ma, Q., Jin, H., Yu, C., and Bense, V. F.: Dissolved organic carbon in permafrost regions: A review, Sci. China Earth Sci., 62, 349–364, https://doi.org/10.1007/s11430-018-9309-6, 2019.

MacDonald, E. N., Tank, S. E., Kokelj, S. V., Froese, D. G., and Hutchins, R. H. S.: Permafrost-derived dissolved organic matter composition varies across permafrost end-members in the western Canadian Arctic, Environ. Res. Lett., 16, 024036, https://doi.org/10.1088/1748-9326/abd971, 2021.

Magnússon, R. Í., Limpens, J., van Huissteden, J., Kleijn, D., Maximov, T. C., Rotbarth, R., Sass-Klaassen, U., and Heijmans, M. M. P. D.: Rapid Vegetation Succession and Coupled Permafrost Dynamics in Arctic Thaw Ponds in the Siberian Lowland Tundra, Journal of Geophysical Research: Biogeosciences, 125, e2019JG005618, https://doi.org/10.1029/2019JG005618, 2020.

Manasypov, R. M., Vorobyev, S. N., Loiko, S. V., Kritzkov, I. V., Shirokova, L. S., Shevchenko, V. P., Kirpotin, S. N., Kulizhsky, S. P., Kolesnichenko, L. G., Zemtzov, V. A., Sinkinov, V. V., and Pokrovsky, O. S.: Seasonal dynamics of organic carbon and metals in thermokarst lakes from the discontinuous permafrost zone of western Siberia, Biogeosciences, 12, 3009–3028, https://doi.org/10.5194/bg-12-3009-2015, 2015.

Mann, P. J., Sobczak, W. V., LaRue, M. M., Bulygina, E., Davydova, A., Vonk, J. E., Schade, J., Davydov, S., Zimov, N., Holmes, R. M., and Spencer, R. G. M.: Evidence for key enzymatic controls on metabolism of Arctic river organic matter, Global Change Biology, 20, 1089–1100, https://doi.org/10.1111/gcb.12416, 2014.

Mann, P. J., Eglinton, T. I., McIntyre, C. P., Zimov, N., Davydova, A., Vonk, J. E., Holmes, R. M., and Spencer, R. G. M.: Utilization of ancient permafrost carbon in headwaters of Arctic fluvial networks, Nat Commun, 6, 7856, https://doi.org/10.1038/ncomms8856, 2015.

Marschner, B. and Kalbitz, K.: Controls of bioavailability and biodegradability of dissolved organic matter in soils, Geoderma, 113, 211–235, https://doi.org/10.1016/S0016-7061(02)00362-2, 2003.

Matveev, A., Laurion, I., and Vincent, W. F.: Winter Accumulation of Methane and its Variable Timing of Release from Thermokarst Lakes in Subarctic Peatlands, Journal of Geophysical Research: Biogeosciences, 124, 3521–3535, https://doi.org/10.1029/2019JG005078, 2019.

Mazoyer, F., Laurion, I., and Rautio, M.: The dominant role of sunlight in degrading winter dissolved organic matter from a thermokarst lake in a subarctic peatland, Biogeosciences, 19, 3959–3977, https://doi.org/10.5194/bg-19-3959-2022, 2022.

McCallister, S. L., Ishikawa, N. F., and Kothawala, D. N.: Biogeochemical tools for characterizing organic carbon in inland aquatic ecosystems, Limnology and Oceanography Letters, 3, 444–457, https://doi.org/10.1002/lol2.10097, 2018.

McDowell, W. H., Zsolnay, A., Aitkenhead-Peterson, J. A., Gregorich, E. G., Jones, D. L., Jödemann, D., Kalbitz, K., Marschner, B., and Schwesig, D.: A comparison of methods to determine the biodegradable dissolved organic carbon from different terrestrial sources, Soil Biology and Biochemistry, 38, 1933–1942, https://doi.org/10.1016/j.soilbio.2005.12.018, 2006.

Murphy, K. R., Stedmon, C. A., Graeber, D., and Bro, R.: Fluorescence spectroscopy and multi-way techniques. PARAFAC, Analytical Methods, 5, 6557–6566, https://doi.org/10.1039/C3AY41160E, 2013.

Murphy, K. R., Stedmon, C. A., Wenig, P., and Bro, R.: OpenFluor– an online spectral library of auto-fluorescence by organic compounds in the environment, Analytical Methods, 6, 658–661, https://doi.org/10.1039/C3AY41935E, 2014.

Muster, S., Heim, B., Abnizova, A., and Boike, J.: Water Body Distributions Across Scales: A Remote Sensing Based Comparison of Three Arctic Tundra Wetlands, Remote Sensing, 5, 1498–1523, https://doi.org/10.3390/rs5041498, 2013.

Mutschlecner, A. E., Guerard, J. J., Jones, J. B., and Harms, T. K.: Phosphorus Enhances Uptake of Dissolved Organic Matter in Boreal Streams, Ecosystems, 21, 675–688, https://doi.org/10.1007/s10021-017-0177-1, 2018.

Nitze, I., Grosse, G., Jones, B. M., Romanovsky, V. E., and Boike, J.: Remote sensing quantifies widespread abundance of permafrost region disturbances across the Arctic and Subarctic, Nat Commun, 9, 5423, https://doi.org/10.1038/s41467-018-07663-3, 2018.

Nusch, E. A.: Comparison of different methods for chlorophyll and phaeopigment determination, Archiv für Hydrobiologie, 14, 14–36, 1980.

Ola, A., Fortier, D., Coulombe, S., Comte, J., and Domine, F.: The Distribution of Soil Carbon and Nitrogen Stocks Among Dominant Geomorphological Terrain Units in Qarlikturvik Valley, Bylot Island, Arctic Canada, Journal of Geophysical Research: Biogeosciences, 127, e2021JG006750, https://doi.org/10.1029/2021JG006750, 2022.

Olefeldt, D., Goswami, S., Grosse, G., Hayes, D., Hugelius, G., Kuhry, P., McGuire, A. D., Romanovsky, V. E., Sannel, A. B. K., Schuur, E. a. G., and Turetsky, M. R.: Circumpolar distribution and carbon storage of thermokarst landscapes, Nat Commun, 7, 13043, https://doi.org/10.1038/ncomms13043, 2016.

Pacoureau, T., Mazoyer, F., Maranger, R., Rautio, M., and Laurion, I.: Shifts in dissolved organic matter and nutrients in tundra ponds along a gradient of permafrost erosion, Arctic Science, 11, 1–17, https://doi.org/10.1139/as-2024-0060, 2025.

Pinheiro, J. and Bates, D.: _nlme: Linear and Nonlinear Mixed Effects Models_, 2023.

Pokrovsky, O. S., Karlsson, J., and Giesler, R.: Freeze-thaw cycles of Arctic thaw ponds remove colloidal metals and generate low-molecular-weight organic matter, Biogeochemistry, 137, 321–336, https://doi.org/10.1007/s10533-018-0421-6, 2018.

Prèskienis, V.: La forte variabilité des émissions de gaz à effet de serre des lacs et des mares de l'Arctique expliquée par la morphologie des plans d'eau, l'activité érosive et la qualité de la matière organique des sols environnants. / The high variability of greenhouse gas emissions from Arctic lakes and ponds explained by the morphology of water bodies, the erosional activity and the quality of organic matter in surrounding soils., phd, Institut National de la Recherche Scientifique, Québec, 186 pp., 2022.

Prèskienis, V., Laurion, I., Bouchard, F., Douglas, P. M. J., Billett, M. F., Fortier, D., and Xu, X.: Seasonal patterns in greenhouse gas emissions from lakes and ponds in a High Arctic polygonal landscape, Limnology and Oceanography, 66, S117–S141, https://doi.org/10.1002/lno.11660, 2021.

Prėskienis, V., Fortier, D., Douglas, P. M. J., Rautio, M., and Laurion, I.: Permafrost degradation and soil erosion as drivers of greenhouse gas emissions from tundra ponds, Environ. Res. Lett., 19, 014072, https://doi.org/10.1088/1748-9326/ad1433, 2024.

R Core Team: _R: A Language and Environment for Statistical Computing_. R Foundation for Statistical Computing, 2024.

Rautio, M., Dufresne, F., Laurion, I., Bonilla, S., Vincent, W. F., and Christoffersen, K. S.: Shallow freshwater ecosystems of the circumpolar Arctic, Écoscience, https://doi.org/10.2980/18-3-3463, 2011.

Rodríguez, P., Ask, J., Hein, C. L., Jansson, M., and Karlsson, J.: Benthic organic carbon release stimulates bacterioplankton production in a clear-water subarctic lake, Freshwater Science, 32, 176–182, https://doi.org/10.1899/12-005.1, 2013.

Roiha, T., Laurion, I., and Rautio, M.: Carbon dynamics in highly heterotrophic subarctic thaw ponds, Biogeosciences, 12, 7223–7237, https://doi.org/10.5194/bg-12-7223-2015, 2015.

Shirokova, L. S., Chupakov, A. V., Zabelina, S. A., Neverova, N. V., Payandi-Rolland, D., Causserand, C., Karlsson, J., and Pokrovsky, O. S.: Humic surface waters of frozen peat bogs (permafrost zone) are highly resistant to bio- and photodegradation, Biogeosciences, 16, 2511–2526, https://doi.org/10.5194/bg-16-2511-2019, 2019.

Smith, E. M. and Prairie, Y. T.: Bacterial metabolism and growth efficiency in lakes: The importance of phosphorus availability, Limnology and Oceanography, 49, 137–147, https://doi.org/10.4319/lo.2004.49.1.0137, 2004.

Spencer, R. G. M., Mann, P. J., Dittmar, T., Eglinton, T. I., McIntyre, C., Holmes, R. M., Zimov, N., and Stubbins, A.: Detecting the signature of permafrost thaw in Arctic rivers, Geophysical Research Letters, 42, 2830–2835, https://doi.org/10.1002/2015GL063498, 2015.

Stubbins, A., Lapierre, J.-F., Berggren, M., Prairie, Y. T., Dittmar, T., and del Giorgio, P. A.: What's in an EEM? Molecular Signatures Associated with Dissolved Organic Fluorescence in Boreal Canada, Environ. Sci. Technol., 48, 10598–10606, https://doi.org/10.1021/es502086e, 2014.

Tank, S. E., Vonk, J. E., Walvoord, M. A., McClelland, J. W., Laurion, I., and Abbott, B. W.: Landscape matters: Predicting the biogeochemical effects of permafrost thaw on aquatic networks with a state factor approach, Permafrost and Periglacial Processes, 31, 358–370, https://doi.org/10.1002/ppp.2057, 2020.

Textor, S. R., Wickland, K. P., Podgorski, D. C., Johnston, S. E., and Spencer, R. G. M.: Dissolved Organic Carbon Turnover in Permafrost-Influenced Watersheds of Interior Alaska: Molecular Insights and the Priming Effect, Front. Earth Sci., 7, https://doi.org/10.3389/feart.2019.00275, 2019.

Vähätalo, A. V. and Wetzel, R. G.: Long-term photochemical and microbial decomposition of wetland-derived dissolved organic matter with alteration of 13C:12C mass ratio, Limnology and Oceanography, 53, 1387–1392, https://doi.org/10.4319/lo.2008.53.4.1387, 2008.

Vidal, L. O., Granéli, W., Daniel, C. B., Heiberg, L., and Roland, F.: Carbon and phosphorus regulating bacterial metabolism in oligotrophic boreal lakes, Journal of Plankton Research, 33, 1747–1756, https://doi.org/10.1093/plankt/fbr059, 2011.

Vonk, J. E., Mann, P. J., Davydov, S., Davydova, A., Spencer, R. G. M., Schade, J., Sobczak, W. V., Zimov, N., Zimov, S., Bulygina, E., Eglinton, T. I., and Holmes, R. M.: High biolability of ancient permafrost carbon upon thaw, Geophysical Research Letters, 40, 2689–2693, https://doi.org/10.1002/grl.50348, 2013.

Vonk, J. E., Tank, S. E., Mann, P. J., Spencer, R. G. M., Treat, C. C., Striegl, R. G., Abbott, B. W., and Wickland, K. P.: Biodegradability of dissolved organic carbon in permafrost soils and aquatic systems: a meta-analysis, Biogeosciences, 12, 6915–6930, https://doi.org/10.5194/bg-12-6915-2015, 2015a.

Vonk, J. E., Tank, S. E., Bowden, W. B., Laurion, I., Vincent, W. F., Alekseychik, P., Amyot, M., Billet, M. F., Canário, J., Cory, R. M., Deshpande, B. N., Helbig, M., Jammet, M., Karlsson, J., Larouche, J., MacMillan, G., Rautio, M., Walter Anthony, K. M., and Wickland, K. P.: Reviews and syntheses: Effects of permafrost thaw on Arctic aquatic ecosystems, Biogeosciences, 12, 7129–7167, https://doi.org/10.5194/bg-12-7129-2015, 2015b.

von Wachenfeldt, E. and Tranvik, L. J.: Sedimentation in Boreal Lakes—The Role of Flocculation of Allochthonous Dissolved Organic Matter in the Water Column, Ecosystems, 11, 803–814, https://doi.org/10.1007/s10021-008-9162-z, 2008.

Walker, D. A., Raynolds, M. K., Daniëls, F. J. A., Einarsson, E., Elvebakk, A., Gould, W. A., Katenin, A. E., Kholod, S. S., Markon, C. J., Melnikov, E. S., Moskalenko, N. G., Talbot, S. S., Yurtsev, B. A. (†), and Team, T. other members of the C.: The Circumpolar Arctic vegetation map, Journal of Vegetation Science, 16, 267–282, https://doi.org/10.1111/j.1654-1103.2005.tb02365.x, 2005.

Ward, C. P., Nalven, S. G., Crump, B. C., Kling, G. W., and Cory, R. M.: Photochemical alteration of organic carbon draining permafrost soils shifts microbial metabolic pathways and stimulates respiration, Nat Commun, 8, 772, https://doi.org/10.1038/s41467-017-00759-2, 2017.

Wauthy, M., Rautio, M., Christoffersen, K. S., Forsström, L., Laurion, I., Mariash, H. L., Peura, S., and Vincent, W. F.: Increasing dominance of terrigenous organic matter in circumpolar freshwaters due to permafrost thaw, Limnology and Oceanography Letters, 3, 186–198, https://doi.org/10.1002/lol2.10063, 2018.

Weishaar, J. L., Aiken, G. R., Bergamaschi, B. A., Fram, M. S., Fujii, R., and Mopper, K.: Evaluation of Specific Ultraviolet Absorbance as an Indicator of the Chemical Composition and Reactivity of Dissolved Organic Carbon, Environ. Sci. Technol., 37, 4702–4708, https://doi.org/10.1021/es030360x, 2003.

Wetzel, R. G., Hatcher, P. G., and Bianchi, T. S.: Natural photolysis by ultraviolet irradiance of recalcitrant dissolved organic matter to simple substrates for rapid bacterial metabolism, Limnology and Oceanography, 40, 1369–1380, https://doi.org/10.4319/lo.1995.40.8.1369, 1995.

Wickland, K. P., Aiken, G. R., Butler, K., Dornblaser, M. M., Spencer, R. G. M., and Striegl, R. G.: Biodegradability of dissolved organic carbon in the Yukon River and its tributaries: Seasonality and importance of inorganic nitrogen, Global Biogeochemical Cycles, 26, https://doi.org/10.1029/2012GB004342, 2012.

Wologo, E., Shakil, S., Zolkos, S., Textor, S., Ewing, S., Klassen, J., Spencer, R. G. M., Podgorski, D. C., Tank, S. E., Baker, M. A., O'Donnell, J. A., Wickland, K. P., Foks, S. S. W., Zarnetske, J. P., Lee-Cullin, J., Liu, F., Yang, Y., Kortelainen, P., Kolehmainen, J., Dean, J. F., Vonk, J. E., Holmes, R. M., Pinay, G., Powell, M. M., Howe, J., Frei, R. J., Bratsman, S. P., and Abbott, B. W.: Stream Dissolved Organic Matter in Permafrost Regions Shows Surprising Compositional Similarities but Negative Priming and Nutrient Effects, Global Biogeochemical Cycles, 35, e2020GB006719, https://doi.org/10.1029/2020GB006719, 2021.

Zhang, X., Hutchings, J. A., Bianchi, T. S., Liu, Y., Arellano, A. R., and Schuur, E. A. G.: Importance of lateral flux and its percolation depth on organic carbon export in Arctic tundra soil: Implications from a soil leaching experiment, Journal of Geophysical Research: Biogeosciences, 122, 796–810, https://doi.org/10.1002/2016JG003754, 2017.